Juha Virtanen

Development of Sensor Integrated and Inkjet-Printed Tag Antennas for Passive UHF RFID Systems

Tampere 2012

Juha Virtanen

Development of Sensor Integrated and Inkjet-Printed Tag Antennas for Passive UHF RFID Systems

Thesis for the degree of Doctor of Science in Technology to be presented with due permission for public examination and criticism in Tietotalo Building, Auditorium TB111, at Tampere University of Technology, on the 21st of December 2012, at 12 noon.

ABSTRACT

Radio frequency identification (RFID) is a form of automated identification technology that is nowadays widely used to replace bar codes in asset tracking and management. Looking ahead to the future, our lives will be surrounded by small, embedded and wireless electronic devices that provide information about everything for everybody through pervasive computing. At the core of this vision lie two key concepts of ubiquitous sensing and the Internet of Things. RFID technology is seen as one of the most prominent technologies of today for the implementation of these future concepts.

Ubiquitous sensing describes a situation, where small embedded sensors monitoring various environmental parameters are found everywhere. The second concept, the Internet of Things, requires that all objects, even the most insignificant everyday items, surrounding us should encompass computing and communication capabilities of some sort. In its simplest form, such computing could be a transponder that allows the unique identification and tracking of the item. Together these future concepts could truly revolutionize our lives by delivering significantly more information from our living environment.

The objectives of this thesis are twofold. Firstly, passive ultra-high frequency (UHF) RFID technology is utilized to develop low cost, completely passive, wireless sensor devices for ubiquitous sensing applications. Secondly, inkjet-printed passive UHF RFID tag antennas are developed and optimization techniques are presented to lower the cost of such tag antenna implementations. The latter objective aims to facilitate the advancement of the Internet of Things by enabling tag antennas to be directly printed on or in to various objects.

As a result of the research work presented in this thesis, three different passive UHF RFID based sensor tags were developed. Two of these designs monitor temperature and one is developed for relative humidity measurements. For the first time, the applicability and accuracy of such passive sensor tags was demonstrated. The results show that UHF RFID sensor tags have potential to be utilized as low cost sensor devices in ubiquitous applications. In addition, this thesis presents methods to lower the costs of inkjet-printed tag antennas. A technique was developed to reduce the ink consumption significantly to produce high performance tag antennas. Moreover, a special type of tag antenna design consisting of very narrow lines was developed. Finally, novel electronic materials were used as tag antenna substrate materials for inkjet-printed tag antennas. The use of a high permittivity ceramic-polymer composite, wood veneer, paper and cardboard were demonstrated. In each case, it was shown that inkjet-printing is a feasible form of fabrication on such materials, producing passive UHF RFID tags with long read ranges. This shows that tag antennas can be inkjet-printed directly on to various items to advance the realization of the Internet of Things.

ACKNOWLEDGEMENTS

Firstly, I want to thank my advisor Adj. Prof. Leena Ukkonen and the Head of the Department of Electronics at Tampere University of Technology Prof. Lauri Sydänheimo for believing in me and giving me the opportunity to complete my doctoral studies as a part of their research group – I will be forever grateful to you for this. I'm also grateful to Prof. Atef Elsherbeni for his support during my research work. Moreover, I want to thank Prof. Elsherbeni and Prof. Fan Yang for giving me enlightening opportunity to visit the University of Mississippi and conduct research with their research group.

My sincerest thanks go to all my co-workers at the Wireless Identification and Sensing Systems Research group and at the Department of Electronics - I always greatly enjoyed working with you all. All my co-authors deserve special thanks for their significant input to my research work. Firstly, I want to acknowledge the support of Dr. Toni Björninen, a great researcher, inspiring professional and a good friend and colleague with whom we have published several high quality publications. I've also had the privilege to work with Abdul Ali Babar, who is a good friend and highly innovative researcher – thanks for all the inspiring discussions and laughs we have had during these recent years. I owe a huge thanks to Dr. Johanna Virkki, who suggested the idea of inkjet-printing on bare veneer. Also, thanks for all the nice discussions and laughs we had by the inkjet-printer. Thanks to Mikko Lauri, a good friend and colleague, for the numerous tips, tricks, assistance and helpful discussions that aided me in the course of my research. A special thanks goes to Dr. Tiiti Kellomäki for her inspiring teachings in RF electronics.

All this would have not been possible without my friends who have inspired me, supported me and provided me the strength to come this far in my life. Thanks especially to Harri, Hermanni, Tommi, Marko and to all my other friends from TUT. Words cannot describe the amount of gratitude I have for my longtime friends Aleksi, Lauri, Matti, Pekka, Petri, Teemu and Timo for all the good times we have had. I'm truly privileged to call you guys my friends – *niin kuin pitääkin*.

Finally, above all, I want to thank my loving fiancée Satu, who I thank for standing by me for all these years, my father Jyrki, mother Marja-Liisa, little brother Jouni and the rest of my family and relatives for their endless support, encouragement and love.

Tampere, October 2012

Juha Virtanen

LIST OF PUBLICATIONS

[P1]   J. Virtanen, L. Ukkonen, T. Björninen, A.Z. Elsherbeni, L. Sydänheimo, "Inkjet-printed Humidity Sensor for Passive UHF RFID Systems," *IEEE Transactions on Instrumentation and Measurement,*, vol. 60, no. 8, pp. 2768-2777, 2011.

[P2]   J. Virtanen, L. Ukkonen, T. Björninen, L. Sydänheimo, A.Z. Elsherbeni, "Temperature Sensor Tag for Passive UHF RFID Systems," *2011 IEEE Sensors Applications Symposium*, pp. 312-317, San Antonio, TX, USA, 22-24 February, 2011.

[P3]   J. Virtanen, F. Yang, L. Ukkonen, A.Z. Elsherbeni, A.A. Babar, L. Sydänheimo, "Dual Port Temperature Sensor Tag for Passive UHF RFID Systems", *Sensor Review Journal (accepted for publication)*.

[P4]   J. Virtanen, J. Virkki, A.Z. Elsherbeni, L. Sydänheimo, L. Ukkonen, "A Selective Ink Deposition Method for the Cost-Performance Optimization of Inkjet-Printed UHF RFID Tag Antennas", *International Journal of Antennas and Propagation,* vol. 2012, Article ID 801014, 9 pages, 2012.

[P5]   J. Virtanen, T. Björninen, L. Ukkonen, L. Sydänheimo, "Passive UHF Inkjet-Printed Narrow-Line RFID Tags," *IEEE Antennas and Wireless Propagation Letters*, vol.9, pp. 440-443, 2010.

[P6]   J. Virkki, J. Virtanen, L. Sydänheimo, M.M. Tentzeris, L. Ukkonen, "Embedding Inkjet-printed Antennas into Plywood Structures for Identification and Sensing," *Invited paper in IEEE International conference on RFID Technology and Applications*, pp. 1-6, Nice, France, 5-7 November, 2012.

[P7]   A.A. Babar, J. Virtanen, V.A. Bhagavati, L. Ukkonen, A.Z. Elsherbeni, P. Kallio, L. Sydänheimo, "Inkjet-Printable UHF RFID Tag Antenna on a Flexible Ceramic-Polymer Composite Substrate," *IEEE International Microwave Symposium*, IMS2012, pp. 1-3, Montreal, QC, Canada, 17-22 June, 2012.

AUTHOR'S CONTRIBUTION

[P1] The author has contributed the publication contents and is the main contributor of the publication text.

[P2] The author has contributed the publication contents and is the main contributor of the publication text. The idea for a patch-type sensor tag was suggested by Prof. Fan Yang and fabrication of the tag prototype was made with Abdul Ali Babar.

[P3] The author has contributed the publication contents and is the main contributor of the publication text.

[P4] The optimization technique was developed by the author. The author fabricated and measured the tag samples and is the main contributor of the publication text. Dr. Johanna Virkki helped with the cross-sectional micrographs.

[P5] The author assembled the inkjet-printed narrow-line tag antenna samples and performed part of the simulations of the narrow-line tag antenna. The author performed all of the measurements made in this study and is the main contributor of the publication text. The narrow-line tag antenna was designed and optimized by Dr. Toni Björninen.

[P6] The author developed the inkjet-printing procedures and methods for wood veneer and also performed the inkjet-printing on wood veneer. The tag antennas presented in this publication are developed and simulated by the author. The author performed most of the measurements which were made in co-operation with Dr. Johanna Virkki who also suggested the idea of plywood-embedded tag antennas. The publication text was written in co-operation with Dr. Johanna Virkki.

[P7] The author developed the optimized method for inkjet-printing and performed the fabrication on the ceramic-polymer substrate. The substrate material was developed and fabricated and the antenna was designed by Abdul Ali Babar. The measurements and the publication text were made in co-operation with Abdul Ali Babar.

CONTENTS

1.   Introduction

"*The most profound technologies are those that disappear. They weave themselves into the fabric of everyday life until they are indistinguishable from it*."
– Mark Weiser

These were the starting words of Mark Weiser's "Computer of the 21st century" article published in Scientific American in 1991 [1]. In his revolutionary article, Weiser described the future of computing and how it is found everywhere. In such pervasive computing, we will be surrounded by small electronic devices, mobile and stationary, which are equipped with some computing capabilities and use wireless or wired to communicate with adjacent devices. This kind of smart environment would unite the virtual and physical worlds together and all the information would be available to everyone by everything. [2]

The concept of pervasive computing might have been just a wild vision of the future at the time of invention, but it is nowadays almost reality. Today our living environments contain numerous devices with computing capabilities, in other words we are surrounded by ambient intelligence. For example, laptops, Internet TV, smart phones, pads, intelligent surveillance systems and remotely controlled home appliances are found almost every home. The approaching dawn of pervasive computing is also highlighted by the arrival of Near Field Communication (NFC) modules to mobile phones [3] and by the revolutionary idea by Google Inc. in the form of their Project Glass [4], which could truly integrate physical and virtual worlds together.

Nonetheless, true pervasive computing, as imagined by Weiser, is still far away. True pervasive computing requires that every device and object, even the simplest ones, should encompass some sort of built-in active or passive *intelligence*. In its simplest form, this *intelligence* is something that allows the environment to track and identify nearby devices or objects or provide some information about the application environment. Most importantly, this *intelligence* should be easily embeddable to objects of everyday use and thus hidden from its users. These are challenging demands in terms of cost and integrability. However, modern Radio Frequency Identification (RFID) technology, among others, has the capabilities to solve some of these challenges. [5] [6]

1.1   Ubiquitous sensing and the Internet of Things

At the heart of pervasive computing lies two key concepts required for the realization of such ambient intelligence. These are namely *ubiquitous sensing* and *the Internet of Things*. The term "ubiquitous" comes from the Latin word *ubique* meaning "everywhere [7]. As such, in ubiquitous sensing, the application environment would consist of sensors

all-around, but hidden from the user. These sensors could monitor different environmental parameters such as the temperature, humidity, air pressure or kinetic parameters like acceleration. The concept of the Internet of Things relates to a scenario, where uniquely identifiable objects could communicate with each other and share information wirelessly [8] [9].

RFID and Wireless Sensor Network (WSN) technologies are currently the most widely recognized enabling technologies for realizing ubiquitous sensing and the Internet of Things [10] [7] [11] [12] [13]. Of the two, RFID has the biggest impact on the realization since it can be used to implement the majority of functions such as the tracing and identification of objects and people wirelessly, without the line of sight, from several meters away using totally passive and low cost electronic tags. If needed, RFID tags can be equipped with a variety of integrated sensors to provide sensory data in addition to the data related to identification purposes. These *sensor tags* can be fabricated with low cost and with reasonable sensor accuracy as it will be shown in this thesis later on. Furthermore, RFID technology is already well standardized and widely used in supply chains in a global scale – a crucial feature for the Internet of Things. Nonetheless, RFID currently lacks the key feature required for a truly pervasive technology: the ability to form ad-hoc networks. This feature is enabled by the integration of WSN to RFID networks. Such visionary networks are called Ubiquitous Sensor Networks (USNs) that could truly enable both ubiquitous sensing and the Internet of Things [14] [15] [16]. In these USNs, RFID based tags could be used as distributed elements for the tracking and identification of assets and for low level item level sensing while WSN based smart nodes could be used for more local high precision sensing and computing.

At the moment communication standards and regulations for both technologies do not allow the direct implementation of USNs. Though a possible solution this problem is being developed by the Institute of Electrical and Electronics Engineers (IEEE) in the form of the IEEE 1451 standard family. The new standard will allow the integration of various *smart sensors* implemented with different technologies, such as RFID and WSN, to be integrated together and with other communication networks [17]. This standardization can be considered as the first steps toward ubiquitous sensing – however implementing the Internet of Things will require further standardization and development of middleware in USNs.

1.2 Overview of the passive UHF RFID system

Radio-frequency identification technology is a growing form of an automated identification that uses electromagnetic interaction to enable objects equipped with radio transponders, i.e. tags, to be identified and tracked wirelessly. RFID systems consist of three main components: tags, readers and reader antennas. Tags are small electronic labels, consisting of an integrated combination of an antenna and a microchip that are attached to the objects under identification. A reader unit is essentially a radio transceiver that is used

to provide the wireless communication link with the tag. The reader antenna is connected to the reader unit and it is used to transform the high frequency signal generated by the reader unit to a wireless electromagnetic wave. The reader unit is linked up with the end-application, e.g. a database that is used to store data linked to the tag's identification code. [18] [19]

RFID systems can be divided based on the type of electromagnetic interaction to near-field systems, which are based on capacitive (electric) or inductive (magnetic) coupling, and to far-field systems, which use propagating electromagnetic waves for communication. Near-field RFID systems operate commonly at 125 kHz or at 13.56 MHz center frequencies, while the far-field systems utilize ultra-high frequencies (UHF), from 300 MHz to 3 GHz. The main practical difference between these systems is in the maximal attainable read ranges, i.e. the maximal distance between the reader antenna and tag at which the tag is still readable. The underlying physics behind near-fields limits the read range of such systems up to few tens of centimeters, while the read range of far-field systems ranges from a few meters up to hundreds of meters depending on the implementation of the tags. [18]

The most common tag implementation in the UHF RFID systems is based on a passive approach, presented in Fig. 1. In the so called passive UHF RFID systems, the tags do not contain any external power supplies, e.g. batteries; instead they receive all their operating power as well as commands from the reader unit wirelessly and use modulated backscattering to communicate back to the reader unit. The communication protocol utilized by these types of tags is standardized under the ISO-18000 family of standards [20].

Passive UHF RFID technology enables cost-efficient solutions to automatically identify and track assets rapidly from long ranges and wide areas. As the identification is based on the coupling of electromagnetic waves, there is no line-of-sight requirement between the tag and reader antenna. This allows the tags to be embedded in protective inlays or even inside the actual asset to provide shelter from the harmful environmental effects. An additional benefit of RFID technology in general is that the IC contains user accessible
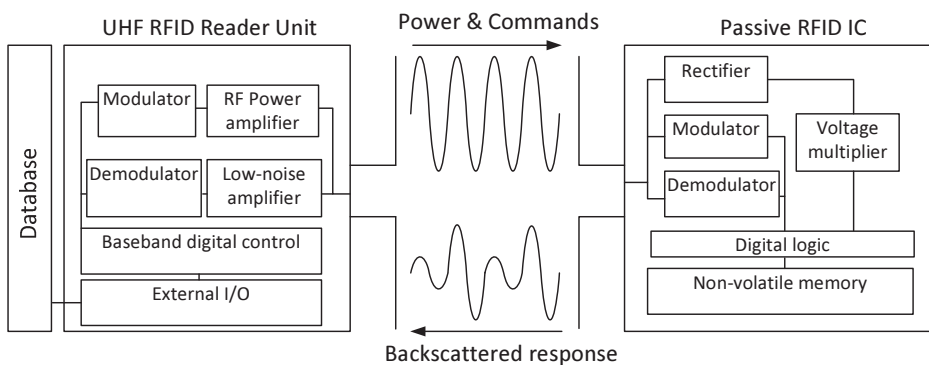

Fig. 1. Overview of the passive UHF RFID system.

memory that allows the storage of data also in the tag itself. These benefits have facilitated the adoption of passive UHF RFID technology and it is nowadays widely used in supply chain management, access control and in item level asset tracking instead of the more traditional bar code. In the future UHF RFID technology will be used in increasing amount of new applications that progress the development toward the Internet of Things and ubiquitous sensing. These include indoor positioning [21], environmental sensing [P1-P3], solutions for wearable ambient intelligence [22] and biomedical applications [23]. [24] [25] [26] [27]

The operation principle of a passive UHF RFID system is as follows. The reader unit generates a high-frequency carrier signal that is transformed by the reader unit's antenna into a propagating electromagnetic wave. This wave is received by the tag antenna, which relays it to the integrated circuit (IC), i.e. microchip. The IC uses its internal rectifiers and voltage multipliers to convert the alternating current to a direct current of sufficient voltage level. Once a sufficient voltage level is achieved, the digital logic in the IC is activated. Now, the tag is ready to receive commands from the reader, if the tag receives a query-command, it responds by sending a 96-bit long unique digital identification code known as the electronic product code (EPC). The response from the tag is generated by the internal modulator in the IC. The modulator, switches between two impedance states, which results in a modulated backscattered response. The communication by backscattering is discussed more in detail in Section 2.3. [24] [28]

Passive UHF RFID systems are subject to regulations concerning their operating frequency and equivalent isotropically radiated power levels (EIRP). These regulations are geographic and are listed in Table 1. The regulations for maximal transmitted power cause the main limitations on the attainable read ranges from passive UHF RFID tags: commonly read ranges vary from a few meters up to fifteen meters although significantly higher read ranges are also attainable using special purpose tags. [29] [30]

Table 1. Overview of regulations for passive UHF RFID systems. [31]

Region	Operating frequency [MHz]	EIRP [W]
Europe	865.6 - 867.6	3.28
United States	902 – 928	4
Japan	952 - 956.4	4
China	840.5 - 844.5 & 920.5 - 924.5	3.28
Russian Federation	866 - 867.6	3.28

Despite the obvious benefits, the global adoption and pervasive use of UHF RFID technology still awaits, due to the many challenges related to it. The foremost challenge is the cost of the implementation. At the moment, the price of the whole system is too great in comparison with bar code systems. Especially the cost of tags needs to be lowered significantly. On the other hand, standardization is problematic since regulations concerning

RFID systems are vastly different depending on the geographical location. In addition, different materials such as liquids and metals cause significant changes in the operation characteristics of tags, e.g. operation frequency shifts, and lead to the need for application-specific tag antennas. Therefore, the need for "universal" or platform-tolerant tags are imminent, i.e. tag that works at all frequencies on all materials, to reduce system complexity [32] [33]. In addition, the integration of UHF RFID tags directly on or in to objects needs novel solutions: at the moment, products are labeled with tags after they leave the production line, causing extra work and costs. In the ideal solution tags would be fabricated directly on the surface of the objects or even inside them at the production line. Other challenges related to the use of RFID in pervasive computing applications are related to tag collisions, data security and need for additional middleware. [34] [35] [36] [37] [38]

1.3   Scope and objective of the thesis

The work presented in this thesis is focused on advancing the deployment of passive UHF RFID technology in applications requiring low cost identification of objects or sensory functions for environmental monitoring. In a larger scale, this work can be seen as a part of providing methods by means of passive UHF RFID technology to realize the concepts of ubiquitous sensing, the Internet of Things and ultimately ambient intelligence by enabling sensory functions and easing the integration of tags directly onto objects.

The scope of this thesis covers the design and development of sensor tags as well as inkjet-printed tag antennas especially for passive UHF RFID systems. The integration of WSNs with RFID technology to realize Ubiquitous Sensing Networks and the further development of ambient intelligence lies outside of the scope of this thesis. The objectives of the thesis can be listed as follows.

- **Enabling sensory functions using passive UHF RFID technology**
  - Development of a passive humidity sensor tag
  - Development of a passive temperature sensor tags
  - Validation of passive sensor tag accuracy
- **Facilitating the integration of UHF RFID low cost tag antennas directly on objects using inkjet-printing**
  - Low cost inkjet-printed tag antennas
    - Studies on optimizing cost-performance
    - New low cost antenna patterns
  - Tag antennas inkjet-printed on novel substrate materials
    - Wood veneer
    - Ceramic-polymer composites
    - Paper and cardboard

1.4   Structure of the thesis

This thesis consists of seven publications and an introductory part to these publications comprising of chapters 1-5. The introductory part is divided into four distinct sections.

Chapter 1, discusses the concepts of pervasive computing, ubiquitous sensing and the Internet of Things. In addition, the basics RFID technology is presented.

Chapter 2, discusses the fundamental parameters of UHF RFID tags. In the first section, an overview is given to the general antenna parameters. This is followed by a short description of the importance of impedance matching in passive tag design. Next, the power transfer and backscattering communication are discussed. Finally, the performance indicators for passive UHF RFID tags are presented.

Chapter 3 focuses on sensor tags implemented using passive UHF RFID technology. In this section, the applications, classifications of UHF RFID based sensor tags as well as benefits and challenges related to completely passive sensor implementations are discussed. Moreover, two realizations of passive UHF RFID sensor tags capable of monitoring environmental humidity [P1] and temperature [P2-P3] levels are presented.

Chapter 4 is related to novel inkjet-printed tag designs and printing techniques for passive UHF RFID systems [P3-P7]. Firstly the section discusses the key benefits and challenges related to inkjet-printing UHF RFID tag antennas. Secondly, three different approaches to minimize production printing costs are presented by means of innovative deposition techniques [P4] and new tag antenna patterns [P5]. Thirdly, it is demonstrated how inkjet-printing can be used to fabricated tags directly onto novel, low cost electronic substrate materials such as wood veneer [P6], ceramic-polymer composites [P7] and paper based materials.

In the fifth and final chapter, the work presented in this thesis is summarized and final conclusions are drawn. Publications [P1-P7] are appended at the end of the thesis.

2. Fundamental parameters of passive UHF RFID tags

This chapter describes the fundamental parameters related to the design of UHF RFID tag antennas for passive systems. First, an overview is given to the general antenna parameters. Next, wireless power transfer using the far-field electromagnetic waves is described and the theory of the communication by backscattering is presented. The final part of the chapter focuses on describing the performance indicators for passive UHF RFID tags.

2.1 Overview of general antenna parameters

An antenna is a special metallic device that radiates and receives electromagnetic waves. These electromagnetic waves are generated by time-varying currents that generate time-varying electric and magnetic fields as stated by the Maxwell's equations. These time-harmonic electromagnetic field equations can be expressed as [39]

$$\nabla \times \bar{E} = -j\omega\mu\bar{H} \tag{1}$$

$$\nabla \times \bar{H} = j\omega\varepsilon\bar{E} + \bar{J} \tag{2}$$

$$\nabla \cdot \bar{E} = \frac{\rho}{\varepsilon} \tag{3}$$

$$\nabla \cdot \bar{H} = 0 \tag{4}$$

$$\nabla \cdot \bar{J} = -j\omega\rho, \tag{5}$$

where $\bar{E}$ is the electric field and $\bar{H}$ the magnetic field intensity vector, ω is the angular frequency, ε and μ are the permittivity and permeability of the medium containing the fields, $\bar{J}$ and ρ are the source current density vector and charge density. The electromagnetic waves propagate spherically away from their source and allow the transfer of power and thus can be used in wireless communication. The complex time-average power emitted by an antenna flowing out through a closed surface s is found generally from [39]

$$P_{rad} = \frac{1}{2}\oiint_s \bar{E} \times \bar{H}^* \, ds, \tag{6}$$

where the integrand inside is defined as the Poynting vector $S = \frac{1}{2}\bar{E} \times \bar{H}^*$.

Field regions

The space surrounding an antenna can be divided into three regions: reactive near-field, radiating near-field and far-field. The division is based on the field structure in each region. The *reactive near-field* is defined as the portion of near-field that immediately surrounds the antenna wherein the reactive field, electric or magnetic, predominates. The

radiating near-field exits in-between the far-field and reactive near-field regions wherein the radiating fields predominate. In general antennas used in the near-field are based on the coupling of electric or magnetic fields and the angular distribution of the fields are dependent on the distance from the antenna. Moreover, as these near-fields are composed of reactive fields, the Poynting vector in a near-field becomes imaginary. Therefore, near-fields do not exhibit any time-average radial power flow, instead the near-field consists of standing waves that store energy. High-frequency (HF) RFID systems operating in near-field regions are based on the coupling of electric or magnetic fields, this limits their read range as the reactive fields attenuate rapidly. [39] [40]

The final region is known as the *far-field*. In the far-field, the angular field distribution is considered independent on the distance from the antenna, the waves resemble local plane waves and the field intensity follows the inverse square law. The Poynting vector of far-field waves becomes real valued, indicating in-phase propagating waves that can be used to transmit power. UHF RFID systems operate by coupling the electromagnetic waves in the far-field as it allows long range readability.

Table 2. Definition of radiation regions [39].

Region	Distance from the antenna	Power density attenuation*
Reactive near-field	0 to $0.62\sqrt{D^3/\lambda}$	$1/r^5$
Radiating near-field	$0.62\sqrt{D^3/\lambda}$ to $2D^2/\lambda$	
Far-field	$2D^2/\lambda$ to ∞	$1/r^2$

* For an ideal dipole antenna

As described, the radiation regions are present at different distances from the radiating antenna. These distances are listed in Table 2, where D is the largest antenna dimension and λ is the wavelength. [39]

Radiation pattern

An ideal isotropical antenna would radiate the fields spherically in every direction; however such antennas are not realizable. Therefore, the radiation intensity from real antennas varies according to the observation point. Hence, special radiation patterns are needed to characterize the antenna radiation as a function of space coordinates. A radiation pattern is formally defined as a mathematical function or a graphical presentation of the radiation properties of an antenna as a function of space coordinates. Usually, the radiation pattern is defined in the far-field, where the field distribution is assumed to be independent on the distance from the antenna. Antennas are reciprocal elements, meaning that the radiation pattern is the same whether the antenna is transmitting or receiving electromagnetic waves. [40]

Radiation patterns can be calculated or measured either by examining the received or transmitted power, i.e. *power pattern*, or variation in the spatial variation of the electric

field amplitude, i.e. *field pattern*, along a constant radius. In most cases, the radiation patterns are normalized using the maximal values of obtained power levels or amplitudes. The *normalized field pattern F(θ,φ)* of the electric field and the *normalized power patterns P(θ,φ)* can be calculated as [39]

$$F(\theta, \phi) = \frac{E(\theta,\phi)}{max(E(\theta,\phi))}, \quad P(\theta,\phi) = |F(\theta,\phi)|^2. \tag{7}$$

The field patterns of linear polarized antennas can be divided into two principal planes: E and H planes. An E plane is the plane containing the electric-field vector and direction of maximum radiation, while H plane contains the magnetic-field vector and direction of maximum radiation. [40]

In practice antennas exhibit two types of radiation patterns: omnidirectional and directional patterns. An omnidirectional radiation pattern is defined as having an essentially nondirectional pattern in a given plane and a directional pattern in any orthogonal plane. A directional pattern on the other hand indicates that the antenna is radiating or receiving power more effectively from some directions than from others. [40]

Directivity and gain

Another parameter to describe the radiation characteristics of an antenna is to define *antenna directivity D*. Antenna directivity is defined as the ratio of the radiation intensity in a given direction from the antenna to the radiation intensity averaged over all directions. In other words, antenna directivity describes how well the antenna focuses its radiated power to a given direction. The radiation intensity needed in the definition of directivity is defined as the power radiated from an antenna per unit solid angle. In the far field, the *radiation intensity U* is given by [39]

$$U(\theta, \phi) = r^2 \cdot \frac{1}{2} Re[S(\theta, \phi)] = U_{max}|F(\theta,\phi)|^2, \tag{8}$$

where r is the distance from the radiator, S is the Poynting vector describing the power density of the radiation and U_{max} is the maximum radiation intensity. The unit of radiation intensity is Watts per solid angle. Using the radiation intensity in Eq. (8), the *antenna directivity D* can be defined as [39]

$$D(\theta, \phi) = \frac{U(\theta,\phi)}{U_{ave}} = \frac{U(\theta,\phi)}{\frac{1}{4\pi}\int_0^{2\pi}\int_0^\pi U(\theta,\phi)\sin\theta \; d\theta d\phi}, \tag{9}$$

where U_{ave} is the average radiation intensity. As it seen, antenna directivity is dimensionless and given by the radiation pattern of the antenna. An isotropic antenna would have a directivity of unity, while all other non-isotropic antennas will exhibit directivities over unity. Usually, antenna directivity is expressed in dBi, which indicates the antenna directivity over the directivity of an isotropic antenna.

Antenna directivity assumes that the radiating antenna is lossless, i.e. it is made out of perfect conductors and is situated in a lossless media. In practice this is not the case and the losses in the antenna structure need to be taken into consideration. These losses are included by the *antenna gain G* [40]

$$G(\theta, \phi) = e_{cd} D(\theta, \phi), \; e_{cd} = \frac{P_{rad}}{P_{in}}, \tag{10}$$

where e_{cd} is the antenna radiation efficiency, which describes the relation between the antenna radiated power P_{rad} and accepted power from the generator P_{in}. Finally, it should be noted that if no specific angles are given for the radiation intensity, directivity or gain, maximum values are implied.

Input impedance

The input impedance of an antenna is defined as the impedance presented by an antenna at its input terminals. The antenna input impedance can be expressed by $Z_a = R_a + jX_a$, where R_a and X_a are the antenna resistance and reactance at the input terminals. The input resistance of the antenna can be divided into two parts $R_a = R_r + R_L$, where R_r stands for the radiation resistance and R_L as the loss resistance. Power dissipated in the radiation resistance represents radiated power, while the power dissipated in the loss resistance is considered to dissipate as heat. [40] [39]

2.2 Impedance matching

The impedance matching between the generator and load, in the case of RFID: the tag antenna and RFID IC, determines the power transfer between them. To achieve the maximal power transfer, the load impedance needs to be the complex conjugate of the generator's internal impedance. Any deviations from this arrangement will lead to additional power losses. Therefore, it is the up most importance to provide good impedance matching between the IC and tag antenna in a passive UHF RFID tag to allow long read ranges.

A passive UHF RFID tag can be represented by a simple equivalent circuit model, shown in Fig. 2. Here, the tag antenna, with an internal impedance of $Z_a = R_a + jX_a$, generates a voltage V_a and power P_{tag}. The tag antenna is connected to a load, the RFID IC with an input impedance of $Z_{IC} = R_{IC} + jX_{IC}$.
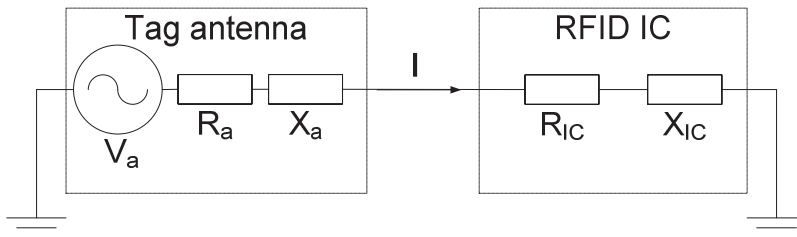

Fig. 2. Equivalent circuit model of a passive tag.

The current in the circuit can be written as

$$I = \frac{V_a}{Z_a + Z_{IC}} = \frac{V_a}{2R_a}(1 - \Gamma) \tag{11}$$

where

$$\Gamma = \frac{Z_{IC} - Z_a^*}{Z_{IC} + Z_a}. \tag{12}$$

Here Γ is the *power wave reflection coefficient* [41], which describes the mismatch between the antenna and IC impedances. The power delivered to the IC is then given by

$$P_{IC} = \frac{1}{2}R_{IC}|I|^2 = \frac{V^2 R_{IC}}{8R_A^2}|1 - \Gamma|^2 = \frac{V_a^2}{8R_A}(1 - |\Gamma|^2) = P_{tag}(1 - |\Gamma|^2), \tag{13}$$

where $|\Gamma|^2$ stands for the power reflection coefficient [42]. The power reflection coefficient describes what fraction of the maximum power available from the generator is not delivered to the load. It can be seen that the maximal power transfer to the IC is achieved when $Z_a = Z_{IC}^*$. An alternative coefficient to describe the power transfer between the IC and tag antenna is the *power transmission coefficient*

$$\tau = 1 - |\Gamma|^2 = \frac{4R_a R_{IC}}{|Z_a + Z_{IC}|^2}, 0 \leq \tau \leq 1. \tag{14}$$

In practice the UHF RFID ICs exhibit nonlinear input power and frequency dependent capacitive input impedances and therefore, to obtain maximal power transfer between the components the tag antenna input reactance needs be inductive [43]. However, the most commonly used tag antenna types, small dipoles, also exhibit capacitive input reactance [39]. Therefore, the input impedance of the tag antenna needs to be transformed to inductive. To achieve such impedance transformation, several types of impedance matching network structures have been developed, e.g. small inductive loops or sections of meander lines positioned in between the RFID IC and tag antenna input terminals. [44] [45]

2.3 Power transmission and backscattering

In passive UHF RFID systems, tags gather all their operating power wirelessly from the continuous signal sent by the reader unit. Once these passive tags have gathered enough power to activate themselves, they use modulated backscattering to generate a response to the reader. This section provides an overview for such power transmission in the passive UHF RFID systems.

A reader unit initiates the communication procedure with a tag by emitting an average power density S, which is given at a distance R by [40]

$$S = \frac{P_{rad}}{4\pi R^2} = \frac{P_t G_t}{4\pi R^2}, \tag{15}$$

where the P_t is the time-average input power accepted by the reader antenna from the power amplifier, G_t is gain of the transmitting reader antenna. The *power received by the tag antenna*, located at distance R from the reader antenna, can be expressed by [40] [46]

$$P_{tag} = S A_{eff,r} \chi_{pol} = \frac{P_t G_t A_{eff,r}}{4\pi R^2} \chi_{pol}, \tag{16}$$

where

$$A_{eff,r} = \frac{\lambda^2}{4\pi} G_{tag} (1 - |\Gamma|^2), \tag{17}$$

and

$$\chi_{pol} = |\hat{p}_{ant} \cdot \hat{p}_{inc}|^2. \tag{18}$$

$A_{eff,r}$ stands for the tag antenna effective aperture, G_{tag} is the gain of the tag antenna and χ_{pol} is the polarization loss factor. The polarization loss factor is determined by the mutual alignment of the tag antenna, $\hat{\rho}_{ant}$, and the incident wave, $\hat{\rho}_{inc}$, electric field polarization vectors. The polarization loss is minimized by using a linearly polarized tag antenna, e.g. dipole, to receive linearly polarized electromagnetic waves transmitted by a linear reader antenna.

Since the passive tags do not contain any radio transceivers that could generate RF power, the tags utilize their tag antennas as scatterers to reflect the incident power from the reader back toward it. The *power reflected by the tag antenna*, from distance R, and received by the reader antenna is given by the radar equation [40] [46]

$$P_{rx,r} = \sigma_r \frac{\lambda^2 G_t P_t G_{tag}}{(4\pi)^3 R^4} \chi_{pol}{}^2, \tag{19}$$

where

$$\sigma_r = \frac{\lambda^2}{4\pi} G_{tag}^2 |1 - \Gamma|^2. \tag{20}$$

The term σ_r is the radar-cross section of a tag antenna, which is used to describe the antennas capability to scatter the incident power from the reader antenna. If the tag antenna's radar-cross section would remain constant, the power from the reader antenna would be reflected back to the reader without any information added by the tag. In order to allow data from the tag IC's memory to be sent, the radar-cross section of the tag antenna needs to change. This allows magnitude and phase variations in the signal received by the reader and thus data exchange. This kind of communication is known as communication by modulated backscattering.

The RFID IC is responsible for modulating the tag antenna's radar-cross section through load modulation. The modulation is implemented by the IC by switching its input impedance between two states, absorbing and reflecting. In the absorbing state the tag antenna and IC are matched while on the reflecting state the components are mismatched and most of the power captured by the tag antenna is reradiated. These impedance states lead to two power wave reflection coefficients Γ_1 and Γ_2. This leads to a *modulated radar-cross section* [47] [48]

$$\sigma_{m,r} = \frac{G_{tag}^2 \lambda^2}{4\pi} m = \frac{G_{tag}^2 \lambda^2}{4\pi} \alpha |\Gamma_1 - \Gamma_2|^2, \tag{21}$$

where α is a modulation loss factor, which depends on the impedance modulation scheme. The types of impedance states used in the load modulation determine if the

backscattered signal is amplitude or phase modulated. As both modulations are possible, the reader units are equipped with IQ-demodulators, which can decipher both types of modulation schemes.

2.4 Performance indicators

The performance of an RFID tag can be examined in different ways. The two most important performance indicators for passive UHF RFID tags are the *transmit power required to activate the tag* and the *maximal read range of the tag*. The transmit power required to activate a tag is often called tag *threshold power*, naturally a low threshold power is desired as it allows long read ranges. The tag read range gives the maximal distance between the reader antenna and tag. Often, in the case of passive UHF RFID tags, it is the power sensitivity of the RFID IC that limits the attainable read range. The abovementioned performance indicators are defined and measured as follows. [48]

The power received by the RFID IC can be derived from Eq.(16) and recalling that $P_{IC}=\tau P_{tag}$

$$ P_{IC} = \tau P_{tag} = \tau G_{tag} \left(\frac{\lambda}{4\pi R}\right)^2 G_t P_t \chi_{pol}. \tag{22} $$

The power required to activate the UHF RFID IC is obtainable from Eq.(22) by changing P_t to P_{th}. The power required to activate the tag from distance R is known as the *tag threshold power* and it is given by

$$ P_{th} = \frac{P_{IC,0}}{\tau G_{tag}\left(\frac{\lambda}{4\pi R}\right)^2 G_t \chi_{pol}}, \tag{23} $$

where $P_{IC,0}$ is the power sensitivity of the RFID IC. For example, the power-sensitivities of the ICs used in the studies presented in this thesis have been in the range of -14 dBm to -18 dBm [P1-P7]. The *forward link read range* is also obtainable from Eq.(16) and assuming a IC power-sensitivity of $P_{IC,0}$

$$ d_{tag,f} = \frac{\lambda}{4\pi} \sqrt{\frac{\tau G_{tag} G_t P_t \chi_{pol}}{P_{IC,0}}} = \frac{\lambda}{4\pi} \sqrt{\frac{\tau G_{tag} \chi_{pol} EIRP}{P_{IC,0}}}, \tag{24} $$

where EIRP is the *maximal allowed equivalent isotropically radiated power*. The term τG_{tag} is also sometimes referred as the *realized gain* of the tag antenna. The EIRP is dictated by the local regulations and $P_{IC,0}$ by the ICs internal design. Tag antenna design wise, the antenna designer can maximize the forward link read range by maximizing tag antenna gain and optimizing the impedance matching between the RFID IC and tag antenna.

In practice, measuring the maximum tag read range is difficult due to environmental multipath propagation and vicinity of dissipative materials. Therefore, in order to obtain
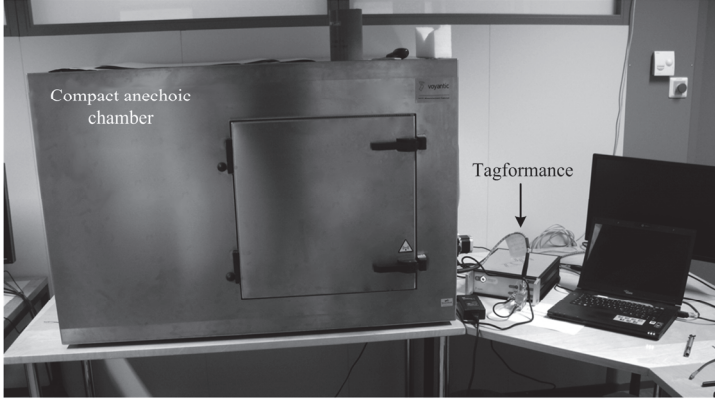
Fig. 3. Measurement equipment used to perform UHF RFID tag performance measurements.

comparable read range results, all the read range results presented in publications [P1-P7] are obtained in artificial free space, i.e. in an anechoic chamber, using Tagformance measurement equipment, shown in Fig. 3. Tagformance is essentially a power and frequency scalable UHF RFID reader unit with some advanced features. Tagformance measurement system is able to calculate the *tag theoretical read range*, which is based on the measured forward link path loss L_{fwd} and tag threshold P_{th}

$$d_{tag,t.f} = \frac{\lambda}{4\pi} \sqrt{\frac{EIRP}{L_{fwd}P_{th}}} . \tag{25}$$

The term theoretical is due to the fact that the measurement is done in free space and the readings are obtained indirectly through the measured threshold power. Therefore, the actual attainable read range behavior can differ from the theoretical values, depending on the application environment.

The path loss L_{fwd} in the forward link is obtained through a calibration step: where the user places a reference tag on the location where the actual tag under test would be placed, next the system performs a threshold sweep on the reference tag. The system stores the information about the precise amount of power required at the reference tag to activate it if it would be connected directly to the transmit port, any deviations from these values are considered as the path loss. The path loss includes the cable losses, polarization losses, reader antenna gain and losses caused by signal attenuation in free space.

Another type of performance metric offered by the Tagformance measurement system for passive UHF RFID tags is the *power-on-tag*. The power-on-tag describes the amount of power required at the tag antenna terminals to activate the tag under test assuming it is equipped with a power matched 0 dBi tag antenna

$$P_{on-tag} = L_{fwd}P_{th}. \tag{26}$$

The benefit of the power-on-tag is that it enables comparable results between tags that are measured from different distances and in different measurement setups. In addition, the effects of possible multipath propagation on the measurement results are minimized.

2.5   Common tag antenna types

A variety of different tag antenna types can be used in passive UHF RFID tags as different applications place varying demands on the tag antennas. The main constraints in general are the cost, size and readability performance (radiation pattern, directivity, etc.) [49]. This section focuses on discussing the three most common types of tag antennas: the dipole, slot and microstrip patch antennas. These common tag antennas are illustrated in Fig. 4 and their main parameters are listed in Table 3.
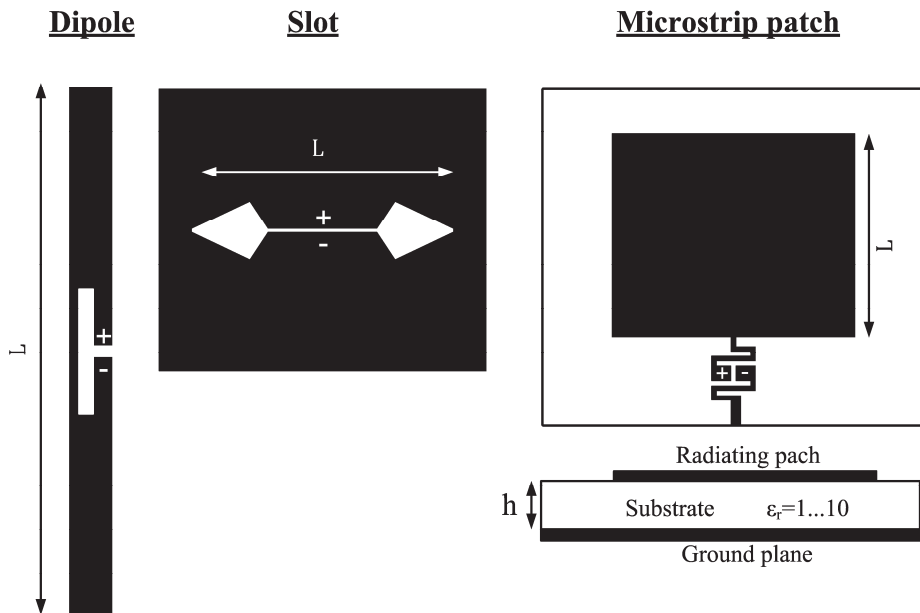
Fig. 4. Common tag antenna types found in UHF RFID tags.

Table 3. Basic parameters for common tag antenna types in passive UHF RFID tags.

	Dipole [40] [39]	**Slot** [40] [39]	**Microstrip patch** [55]
Directivity	2.15 dBi	2.15 dBi	4-9 dBi
Radiator length L	$<\lambda/4$	$<\lambda/4$	$<\lambda/4$
Radiation pattern	Omnidirectional	Omnidirectional	Directional
Input reactance*	Capacitive	Inductive	Inductive
Cost	Low	Intermediate	High

* Typically at frequencies below self-resonance.

Dipole antennas are the most widely used type of tag antennas, e.g. in [P1, P3-P7], since they can be fabricated flexible with low costs and they offer omnidirectional readability in the H plane. The low fabrication costs of dipoles are due to their simple planar construction and small foot prints. Usually, the lengths of dipole antennas found in UHF RFID tags are less than quarter wavelength long; however, the length and foot prints can be miniaturized below this using different folding or loading techniques [50]. The downside of the dipole antenna is that its input reactance is capacitive at frequencies below its self-resonance, which is usually the frequency range where it is used in RFID applications. Therefore, impedance matching techniques need to be utilized to provide good tag readability [44]. In addition the input impedance and radiation characteristics of a dipole are strongly affected by nearby dielectric and conductive materials. This can create readability problems and to obtain maximal readability dipole tag antennas need to be optimized for specific material types. [24]

A second common type of planar tag antenna is a slot antenna, e.g. in [P2]; [51] [52], where the radiation is produced by a slot in a larger metallic plane. The slot antenna is also known as the complementary dipole as it has similar properties as the dipole, but with a few exceptions. Firstly, the input reactance of the slot antenna is inductive at frequencies below its self-resonance. This removes the need for additional impedance matching networks as long as the shape of the slot is optimized to produce enough inductance. Another difference is that the principal planes of the slot are orthogonal compared to the dipole. The drawback of the slot antenna is that it usually requires significantly larger foot prints as the dipole. This is due to the fact that the metallic plane around the radiation slot, which is commonly around quarter wavelength long, needs to be much larger than the width and length of the slot. The size constraint and the higher fabrication costs due to it place limitations on the applicability of slot antennas. [40] [39]

The third type of common tag antenna found in passive UHF RFID tags is the microstrip patch antenna, e.g. in [P3]. The microstrip patch antenna consists of a radiating patch on a substrate material, which is backed by a larger ground plane. Commonly, the length of the radiating patch found in passive UHF RFID tags is around or below a quarter wavelength. However, in order to achieve good performance, the overall size of the antenna is larger due to the demands of the ground plane: The ground plane needs to larger than the radiating patch to accommodate the fringing fields [53]. The overall size of the antenna can be miniaturized by increasing the permittivity of the substrate material or by slotting the radiating patch [50]. Usually the input reactance of a patch antenna is inductive, though in some applications additional impedance matching networks are needed for good tag performance. The main benefit of the patch antenna is that it exhibits high directivity, which allows long attainable read ranges. Moreover, the ground plane of the patch is electrically isolating the antenna from the materials behind the ground plane. Therefore, patch antennas are especially used in on-metal applications or on top of highly dissipative materials [54]. On the downside, the fabrication costs of patch antennas are usually high. [24] [55]

3. Passive sensor integrated UHF RFID tags

Ubiquitous sensing can be achieved by the wide spread utilization of sensor devices everywhere. The challenges related to such scenario are mainly the overall cost and integrability of the sensors to the application environment and objects. Passive UHF RFID technology can solve the cost and integrability issues in many cases as it can be utilized to enable low cost passive sensors that do not need any maintenance procedures. Such sensor tags can be made compact, which eases their integrability to the objects of everyday life. Moreover, the long read range enabled by the use of UHF RFID technology reduces the number of required reader units and thus lowers overall system cost in comparison with sensor systems based on HF RFID technology.

3.1   Implementation methods

Passive UHF RFID sensor tags can be implemented using different methods. In this context, the implementation method is related to the integration of the sensor element to the UHF RFID tag. The different methods for integrating sensors into passive UHF RFID tags can be listed as follows.

- *Tag antenna based sensing*. The lowest cost implementation: the tag antenna is used as the sensor. Thus, no specific sensors, such as discrete components are required. Tag antenna based sensing can be divided into two subcategories of *self-sensing* and *antenna-integrated sensors*. In self-sensing, no specific sensor materials are utilized, i.e. ordinary tags can be used as sensors. In the antenna-integrated sensors, a specific sensor element, usually a material with electrical properties dependent on the physical quantity under sensing, are added as parts of the tag antenna. [P1-P4]; [56] [57] [58] [59]
- *External discrete sensors*. Discrete sensor components are placed in series or in parallel with the RFID IC and the tag antenna. [60] [61]
- *Sensor integrated RFID ICs.* The sensor components are integrated directly into the RFID IC. [62] [63] [64]
- *Microcontroller based smart sensors.* An advanced sensor tag that is equipped with a microcontroller instead of an RFID IC. The improved computing capabilities of a microcontroller allow the use of multiple sensors with better resolution and accuracy. [65]
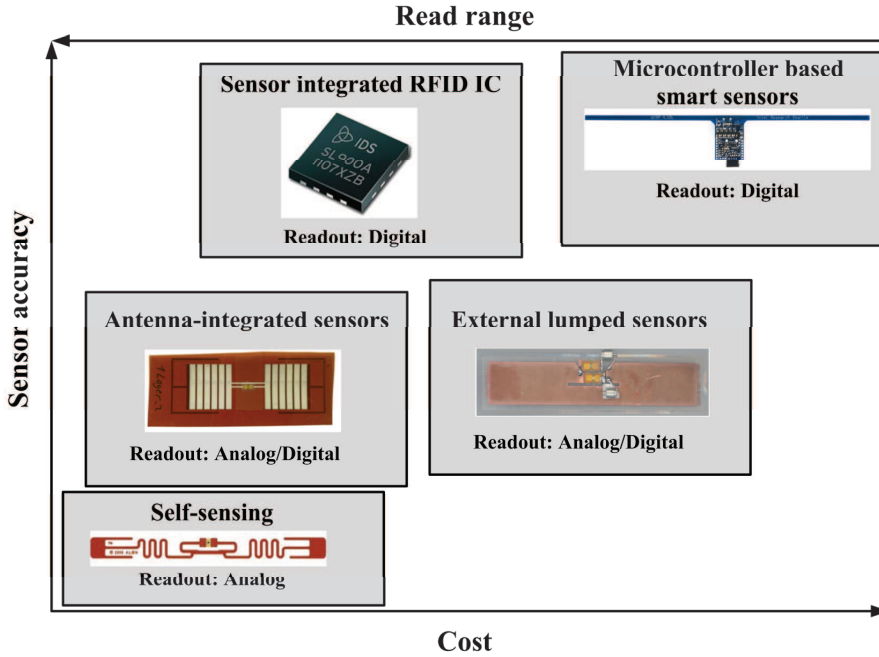
Fig. 5. Classifications of implementation methods of passive sensor tags based on UHF RFID technology.

The sensor integration method has a major effect on the sensor and tag performance and on to the overall cost of the sensor tag: as the complexity of the sensor tag increases, the fabrication costs and sensor performance are usually increased, while the maximal read range of the tag is decreased. These trade-offs are approximated in Fig. 5. In environments with true ubiquitous sensing capabilities, all implementation methods of passive sensor tags will be needed. The sensor tags utilizing tag antenna based sensing would be deployed in macro sensing, due to their low cost. Sensor tags with sensor integrated RFID ICs, external sensor components and microcontrollers would be used in more sparsely, in applications requiring higher levels of resolution and accuracy. [66]

3.2   Applications

In a true ubiquitously sensed world, passive sensor tags would be used everywhere. Their tasks would vary from monitoring the temperature local small objects to supervising the air quality around large areas. This section, presents some examples of possible applications for sensor tags to illustrate their potential benefits. As examples, applications from logistics, healthcare and smart homes are discussed for sensor tags based on passive UHF RFID technology.

3.2.1 Logistics

Supply chain management is currently the biggest application of regular UHF RFID tags worldwide. Integrating sensors into these tags would bring new functionality to the supply management systems. Firstly, sensor tags can enable the monitoring of product condition at the item level. For example, equipping perishable products with sensor tags at the packaging line, allows the supervision of temperatures and humidity levels experienced by the product. This is especially beneficiary in applications where there is a need to guarantee the completeness of cold chains to improve product quality and safety. On the other hand, sensor tags can be used with valuable products to monitor the shock and vibration levels experienced by them [12] [67]. In addition, sensor tags can be used in the automatic detection of product tampering. Equipping tags, for example, with mechanical sensors that detect if the product package has been breached, aids in the battle against smuggling and counterfeiting.

3.2.2 Healthcare

Monitoring of treatment quality regardless of the location of the patient is one of the biggest benefits of sensor tags if utilized within the healthcare sector. These sensor tags could monitor patient's physiological conditions wirelessly all-around the clock if needed. They could, for example, monitor the heart rate, blood pressure and detect if the patient falls or stays still for too long [67]. Occurring seizures or other symptoms would be detected in real time and patients could be located instantly. The low cost of RFID-based sensor tag devices would allow patients with and without chronic diseases to be tagged. Detection of fatal illnesses can be seen as an additional functionality especially for patients belonging with the risk of developing such diseases. For example, small sensor tags could be implanted inside humans using stents or by performing small surgeries. These sensor tags could then be used to detect possible of brain edemas or stenosis inside blood veins [68]. Thirdly, the monitoring and quality control of medication can be made more accurate by the use of sensor tags. Sensor tags can aid medical personnel in the monitoring of medication by logging which medicine and the amount of dosage the patient has consumed. Situations, where the patient has received wrong mediation or an overdose can be therefore avoided. On the other hand, since sensor tags can be integrated with individual packages of medicine, the quality of the medicine can be also controlled. This is achieved by logging the temperature, humidity and possible UV exposure of the medicine using embedded sensor tags in the packages [69].

3.2.3 Smart homes and environments

Passive sensor tags could be utilized also in homes and in other environments to improve the quality of life by aiding people in their daily activities or by quarantining healthy and safe living environments. For example, sensor tags, with sensors for the temperature, humidity or gas monitoring, could be embedded in various structures, such as floors, walls

and ceilings. These tags would be used to minimize energy consumption [70]; [P2-P3], to provide early warnings of possible structural damages, e.g. water damages [P1] or to warn about the presence of toxic gases [71]. Another crucial feature of pervasive computing is its ability to monitor, track and identify activities performed by humans in different environments. Features such as these are enabled by UHF RFID based sensor tags [72] [73]. For example, sensor tags with pressure sensors embedded in the floors of houses could detect the location of humans or animals alike. Likewise, sensor tags, as well as ordinary RFID tags, could be used to detect which objects are used or to locate objects needed by the users [74]. Moreover, sensor tags could be used to provide information about the state of things to other smart devices such as home appliances or autonomous robots [75].

3.3 Tag antenna based sensing: theory and case studies

The most straightforward and lowest cost approach to implement passive sensor tags is to utilize the tag antenna as the sensor itself, i.e. *tag antenna based sensing*, to detect changes in the electrical properties of surrounding materials and objects or changes in some physical parameters. In the simplest implementations even ordinary passive UHF RFID tags, without any specific sensor components, can be used as sensor tags. Such tags used for sensing applications are referred to as *self-sensing*. Self-sensing tags can be used to detect changes in the electrical properties of objects on which they are attached to. This enables sensing of such things as detecting the amount of substances inside containers or the detection of conductive metals [76]. [76]

However, in many cases the self-sensing nature of UHF RFID tags is not capable enough to be used to detect certain physical phenomena. For example, detecting the ambient temperature, humidity, UV-radiation, strain or different types of gasses is not possible by just using self-sensing tags. In such cases, a specific sensor element needs to be added to the tag design. In the so called *antenna-integrated* sensor tag designs, a specific sensing element, material or structure, is integrated into the antenna itself or into the substrate material of the tag.

3.3.1 Intrinsic sensing mechanisms

Passive sensor tags utilizing tag antenna based sensing can monitor environmental parameters throughout either the *material loading* of the tag antenna or through tag *antenna deformation* in a manner illustrated in Fig. 6. Exploiting material loading as the sensing mechanism allows the detection of changes in the electrical properties of materials surrounding the tag antenna. Material loading can be utilized, for example, in the detection of ambient temperature, humidity or gasses if a special type of tag antenna substrate material, which reacts to these parameters by changing its permittivity, permeability or conductivity is utilized [P1-P3]. The material loading causes redistribution of electric and magnetic energy levels in the reactive near field of a tag antenna. This redistribution is specifically caused by the permittivity, permeability and conductivity of the
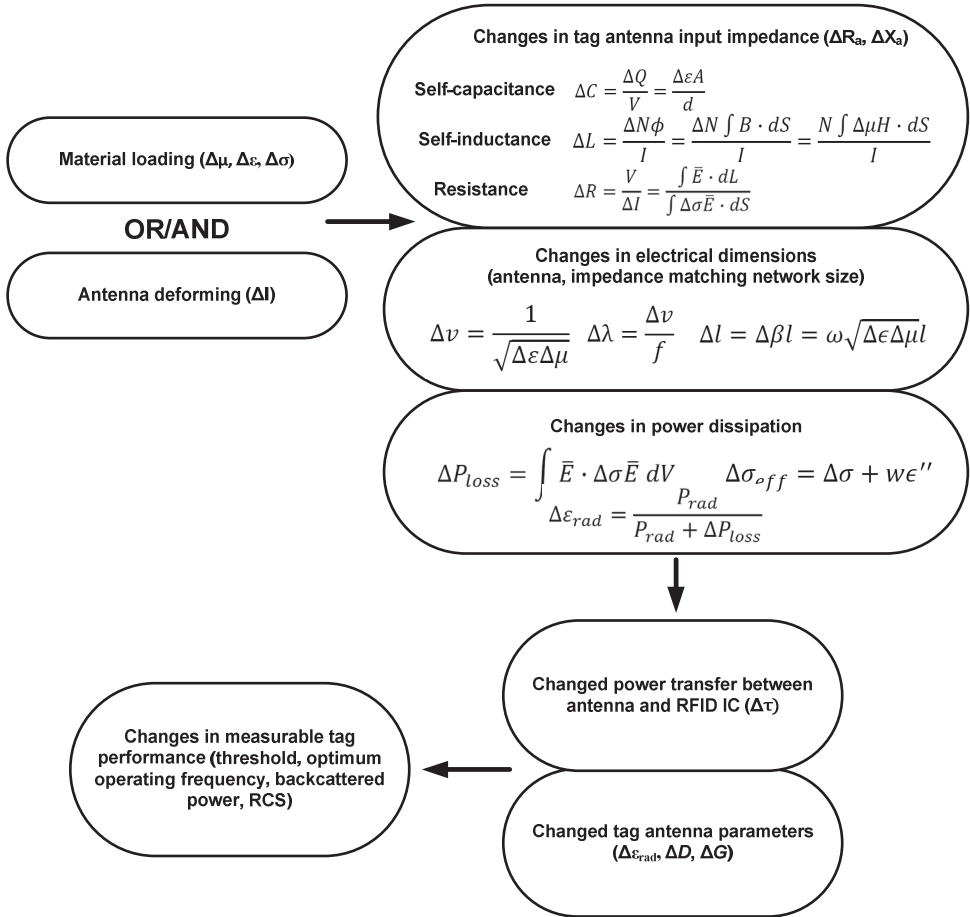
Changes in tag antenna input impedance (ΔR_a, ΔX_a)

Self-capacitance $\quad \Delta C = \dfrac{\Delta Q}{V} = \dfrac{\Delta \varepsilon A}{d}$

Self-inductance $\quad \Delta L = \dfrac{\Delta N\phi}{I} = \dfrac{\Delta N \int B \cdot dS}{I} = \dfrac{N \int \Delta \mu H \cdot dS}{I}$

Resistance $\quad \Delta R = \dfrac{V}{\Delta I} = \dfrac{\int \bar{E} \cdot dL}{\int \Delta \sigma \bar{E} \cdot dS}$

Material loading ($\Delta \mu$, $\Delta \varepsilon$, $\Delta \sigma$)

OR/AND

Antenna deforming (ΔI)

Changes in electrical dimensions (antenna, impedance matching network size)

$$\Delta v = \frac{1}{\sqrt{\Delta \varepsilon \Delta \mu}} \quad \Delta \lambda = \frac{\Delta v}{f} \quad \Delta l = \Delta \beta l = \omega \sqrt{\Delta \epsilon \Delta \mu} l$$

Changes in power dissipation

$$\Delta P_{loss} = \int \bar{E} \cdot \Delta \sigma \bar{E} \, dV \quad \Delta \sigma_{eff} = \Delta \sigma + w\epsilon''$$
$$\Delta \varepsilon_{rad} = \frac{P_{rad}}{P_{rad} + \Delta P_{loss}}$$

Changed power transfer between antenna and RFID IC ($\Delta \tau$)

Changes in measurable tag performance (threshold, optimum operating frequency, backcattered power, RCS)

Changed tag antenna parameters ($\Delta \varepsilon_{rad}$, ΔD, ΔG)

Fig. 6. Tag antenna self-sensing mechanisms and their effect on the measurable tag performance.

material placed in the reactive near field. The effect of reactive near field loading leads to alterations in the current distribution in the antenna structure.

Deforming the tag antenna can be used especially to detect various physical changes such strain or pressure [77]. This sensing mechanism is based on the tag antenna deformation, i.e. antenna dimensions are changed, by the parameter that it sensed. For example, to monitor strain, the substrate material can be made elastic. The reshaping can increase or decrease the physical length, width or thickness of the antenna, causing changes in the current distribution.

Both sensing mechanisms inflict various changes in the tag antenna input impedance and gain. The changes in the tag antenna's input impedance are visible both in the real and imaginary parts [78]. The real part of the input impedance is affected due to changes in the radiation resistance, while the imaginary part is altered due changes in self-capacitance and self-inductance produced by the geometry of the tag antenna and the impedance matching network due to changes in the electric and magnetic fields as well as in

the electrical length of the components. Tag antenna directivity is affected by the changes in the electrical length of the tag antenna and impedance matching network: electrical length is increased as the tag antenna is loaded with dielectric materials or as the tag is stretched. Also, the radiation efficiency is affected by the material loading if dissipative materials are loading the antenna or if the antenna is deformed.

Ultimately, the changes induced by either the material loading of antenna deforming are visible in the measurable tag performance indicators, e.g. threshold power, optimum operating frequency, read range, and thus allow the wireless readout of sensor data.

3.3.2 Wireless readout of sensor data

The sensor data from passive sensor tags utilizing tag antenna based sensing is obtained wirelessly by measuring certain tag performance indicators, for example tag threshold or backscattered power. The key is to link these performance indicators with the sensor stimulus, e.g. temperature or humidity, by obtaining the specific sensor transfer function through calibration. After calibration, the magnitude of sensor stimulus is obtainable by measuring the tag performance metric and applying the known transfer function.

Two types of wireless sensor data readout methods exist. The first approach is based on measuring the magnitude of a measurable tag performance indicator, e.g. threshold power or backscattered power level, at a certain frequency. In an alternative approach, the optimum operating frequencies are measured. Here, the optimum operating frequency point refers to the frequency point at which the measurable tag performance indicator is at its optimal level, e.g. the lowest threshold power level. The creation of the transfer function from both readout methods is illustrated in Fig. 7.

Both readout methods have their benefits and drawbacks. The benefit of the magnitude based method is that requires only transmit power sweeping capabilities from the reader unit, allowing for low cost system components, while the readout method based on the frequency plane on the other hand needs both power and frequency sweeping capabilities. The main drawback of the magnitude based readout is that it dependent on the distance between the reader and sensor tag, thus only static measurements are possible. On the other hand, the readout based on the optimal operating frequency is not dependent on the distance and allows dynamic measurements.

Passive sensor tag performance can be characterized mainly by the sensitivity, accuracy, dynamic range and resolution of the sensor. The two latter ones are limited by the regulations concerning passive UHF RFID systems as well as by the reader unit hardware. The dynamic range of the magnitude based readout is limited by the EIRP levels while the allowable bandwidth limits the dynamic range of the optimum operating frequency method. The sensor resolution, i.e. the smallest measurable difference in the obtained sensor stimulus, is mainly limited by the reader hardware. In the magnitude readout, the minimum transmit and received power steps limit resolution while in the optimum operating
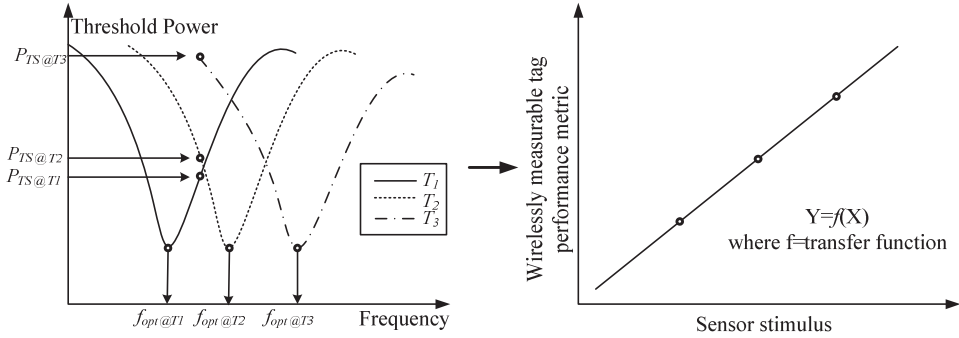
Fig. 7. Illustration of the calibration procedure. The sensor is exposed to different amount of sensor stimulus T1-T3. The tag performance indicators are measured at each stage, which allows the creation of transfer function linking tag performance metric to the sensor stimulus.

frequency point readout, the minimum transmit and received power steps as well as the smallest transmit frequency step affect the readout resolution.

The main challenges related to the use of sensor tags utilizing tag antenna based sensing are induced by the disruptive environmental factors. These factors are multipath propagation, unwanted tag antenna loading and mutual coupling with adjacent tags. These factors cause changes to the sensor transfer function, which is usually characterized in the absence of the harmful environmental factors. Thus, false sensor readings are possible if special care is not taken into consideration.

In order to provide added robustness against the distortions by the application environment two improved readout methods have been developed. In [76], the authors suggest that the ratio between the threshold power and backscattered power levels should be used to extract sensor data. The benefit is that ideally, the effects of reader antenna to sensor tag distance and multipath propagation are removed. An alternative novel readout method called a dual port sensing concept for more robust sensor data readout is suggested in [P1]. The readout method in [P1] is based on equipping the sensor tag with two ports: a sensor port and a reference port. The sensor port, an RFID IC, is connected to a tag antenna which is affected by certain stimulus, while the reference port is connected to an antenna immune to the stimulus. This allows the measurement of relative differences in between the port operating parameters. The advantage of this readout method is that the effects of parasitic tag antenna loading by the surrounding materials and adjacent tags are minimized as both tag antennas are exposed to similar de-tuning effects. In other words, the relative differences in the operating characteristics should remain the same. Alternatively, the reference tag can be used to perform on-site calibrations to minimize the effects of multipath propagation and parasitic material loading.

An additional method to increase sensor tag robustness toward environmental interference is to use retrodirective antenna topologies [79] [80] to reduce the tag's threshold power dependency on the angle of incidence of power from the reader unit. This allows sensor tags to be queried from a wider reader antenna to tag angles.

3.4　Case studies

Passive humidity sensor tag

A passive humidity sensor tag, shown in Fig. 8, was developed in [P1]. The sensor tag was especially designed to be embedded inside or in between walls, floors and ceilings to monitor their humidity levels. This would allow the early detection of possible water damages. The sensor tag could be also used to detect changes in air humidity. The passive humidity sensor tag is equipped with a dipole-type tag antenna and Higgs-3 passive RFID IC from Alien Technology. Kapton® HN500, 125 µm thick a polyimide film is used as the tag substrate. The overall dimensions of the tag are 106 mm by 39 mm.

The humidity-sensing feature of the tag is based on tag antenna material loading by its polyimide substrate material Kapton® HN. Polyimides have high water absorption rates and once they absorb moisture from the air, their permittivity changes. The change in the permittivity of polyimides is due to a hydrolysis effect, which causes the polyimid's carbon-nitrogen bonds to break, allowing for greater electrical polarization [81]. The dependency between the relative permittivity of Kapton HN $\varepsilon_r(H)$ and relative air humidity H is given by

$$\varepsilon_r(H) = 3.05 + 0.008 \times H. \tag{27}$$

The humidity-dependent substrate permittivity is transformed into humidity-dependent capacitance produced by the novel two sided tag antenna design that utilizes a series of parallel plate capacitors. The increased substrate permittivity loads the capacitors, altering the input impedance of the tag antenna accordingly. Ultimately, this leads to a humidity-dependent tag threshold power.

The overall dimensions and the amount of the parallel plates were optimized to produce maximal changes in the input impedance of the tag antenna, while offering good impedance matching. To increase the read range of the tag, additional length was added to the
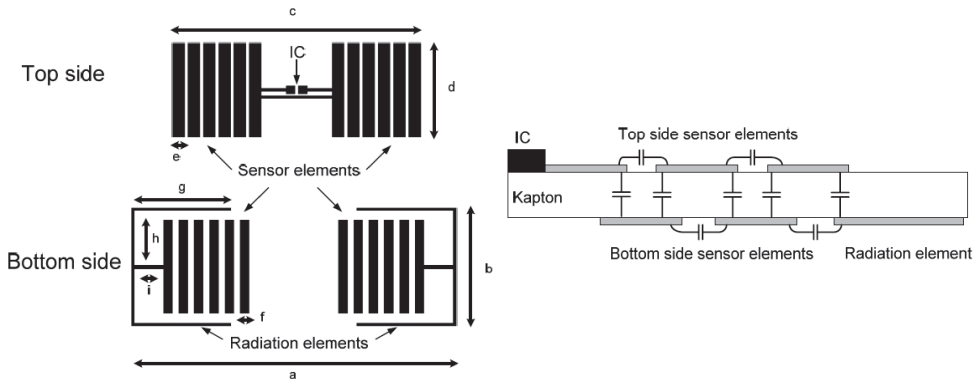

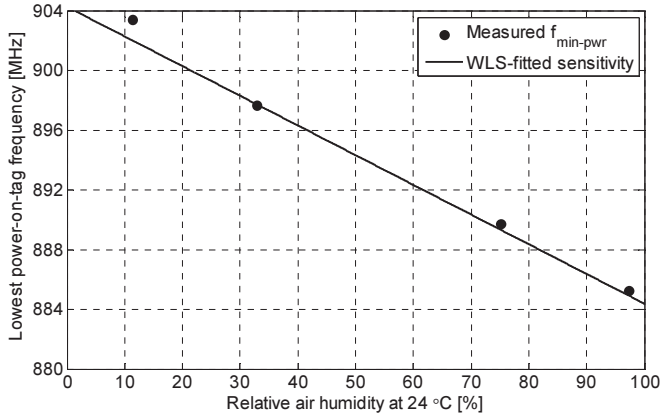**Fig. 8.** Structure of the passive humidity sensor tag. [P1].

Fig. 9. Measured humidity-sensitivity and theoretical read range at 24 ˚C in different relative humidity levels. [P1].

dipole arms to increase the tag antenna gain. Finally, a T-type impedance matching network was added to prove complex-conjugate matching with the input impedance of the RFID IC.

The sensor tag was fabricated on the Kapton® HN film using inkjet-printed Harima NPS-J silver nanoparticle ink. Inkjet-printing was needed as the accurate alignment of the opposing parallel plates was crucial for correct operation in terms of operation frequency and humidity-sensitivity. The humidity sensor tag could be also fabricated using copper. This would increase the attainable read ranges as copper has higher conductivity than the silver nanoparticle ink (33 MS/m vs. 58 MS/m).

A transfer function, linking the optimum power-on-tag frequency point and ambient air humidity was created by a series of humidity controlled measurements in an anechoic chamber. The characterization was done at 24 ˚C in four different relative air humidity levels, 11%, 33%, 75% and 97% using saturated salt solutions with different equilibrium relative humidity levels [82]. The relation between the lowest power-on-tag frequency and relative air humidity was found to be a linear function given by

$$f_{min-pwr} = (-0.1988 \times H + 904.2757) \text{ MHz}. \tag{28}$$

The transfer function is also presented in Fig. 9. The measured sensor performance parameters are listed in Table 3.

Table 4. Measured sensor performance parameters [P1].

Sensitivity	Accuracy	Resolution
198.8 kHz/%RH	± 4.0 %RH	0.5 %RH*

* with 100 kHz transmit frequency steps

The theoretical read range of the passive humidity sensor tag was also measured as a function frequency at different air humidity levels. The maximal read range of the sensor tag was found to vary between 7.6 meters and 8.7 meters in free space.

Passive dipole-type temperature sensor tag

A novel passive dipole-type temperature sensor tag was developed in [P2]. The temperature sensor, shown in Fig. 10, tag finds applications in structural and object temperature monitoring. Thus, it could be used ubiquitously inside walls and floors in homes, to detect the surrounding temperature. Linking this sensor data with the central heating system could be used to reduce energy consumption in smart home applications. Alternatively, it can be used for cold chain monitoring in supply chains.

The passive temperature sensor uses a passive Higgs-3 RFID IC and a copper made dipole-type tag antenna as its main components. The impedance matching is implemented using sections of meander lines and T-type matching. Distilled water contained inside a container made out of polymer is situated on top of the impedance matching section. Low cost FR-4 was used as the tag substrate. The overall dimensions of the tag are 96 mm by 32 mm.

The operation principle of the sensor tag in [P2] is based on the loading of the tag antenna's impedance matching network with distilled water. Distilled water is an excellent ultra low cost and environmentally safe temperature-sensing substance as its permittivity is a linear function of temperature at the global UHF RFID band [83], see Fig. 10. Using distilled water does not cause significant radiation losses and allows long attainable read ranges. The range of measurable temperatures is limited by the freezing and boiling points of water. Although, the use of water was demonstrated in [P2], any other low loss materials with permittivity variations due to the temperature could be used.

The varying permittivity of water is sensed by the sections of meander-lines and T-type impedance matching network. As the permittivity of water changes, the self-capacitance
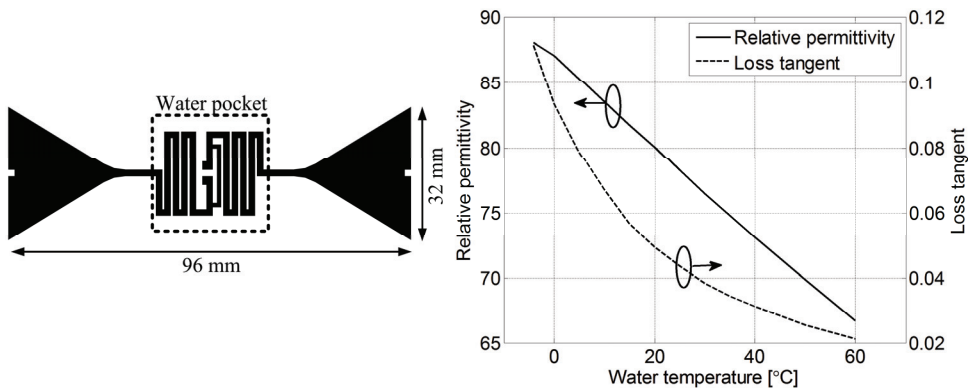

Fig. 10. One the left: layout of the sensor tag. On the right: dielectric properties of distilled water at 900 MHz [82]. [P2]
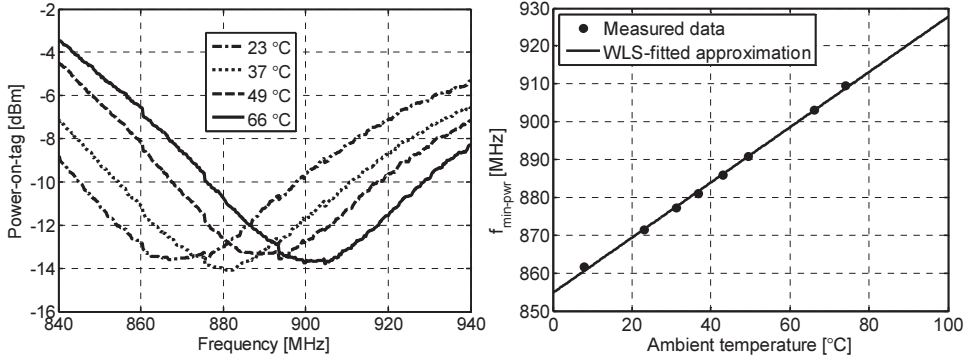
Fig. 11. A) Measured power-on-tag in different ambient air temperatures. B) Transfer function between sensor output and ambient temperature. [P2]

and inductance produced by these sections is altered. Thus, the power transfer between the tag antenna and RFID IC is temperature-dependent, allowing for a wireless measurement of temperature using the threshold power or backscattered power. The measured power-on-tag and the obtained transfer function are presented in Fig. 11.

In [P2], the frequency point of the lowest power-on-tag, i.e. the optimum operating frequency point, was used to monitor changes in the ambient air temperature. The dependency of the frequency of the lowest power-on-tag level was characterized as a function of ambient temperature in an anechoic chamber. The function relating the frequency point of the lowest power-on-tag to the temperature was found to be linear and given by

$$f_{min-pwr} = (0.7295 \times T + 854.7220)MHz. \tag{29}$$

The measured sensor performance parameters for the dipole type-temperature sensor tag are listed in Table 3.

Table 5. Measured sensor performance parameters [P2].

Sensitivity	Accuracy	Resolution	Response time
729.5 kHz/°C	± 0.5°C	0.14 °C*	16 s/°C**

* with 100 kHz transmit frequency steps
** in still air

The dipole antenna allows the temperature tag to be read omnidirectionally in the H plane from a maximal distance of 7.5 meters. The read range of the sensor tag is varied by approximately 0.5 meters depending on the temperature.

Passive dual port temperature sensor tag

A further developed temperature sensor tag is presented in [P3]. Its capability to sense temperature is also enabled by the material loading by distilled water or by any other material with a temperature-dependent permittivity. The sensor tag exploits the "dual port

sensing" concept presented in Section 3.3.2 and its structure is presented in Fig. 12. The overall dimensions of the sensor tag are 90 mm by 78 mm by 6.8 mm.

The dual port temperature sensor tag consists of two tags integrated together. The temperature is sensed by a patch-type tag antenna, which has a distilled water filled cavity within its substrate. A slot antenna attached to the backside of the patch antenna acts as the reference. Both tag antennas are equipped with a Higgs-2 passive UHF RFID ICs. The IC connected to the patch is called the sensor port and the IC connected to the slot is known as the reference port. The changes in the temperature are obtained by measuring the relative differences in the operation characteristics of the two ports.

The use of high permittivity water allows significant miniaturization of the patch. Usually, the sizes of patch antennas are around $\lambda/2$, but the use of high permittivity water and substrate allows reduces the size to around $\lambda/5$. The impedance matching between the patch antenna and Higgs-2 RFID IC was implemented with meander lining. The patch antenna was fed directly from the edge of the patch since it resulted in a sufficient amount of inductive reactance. The drawback of this solution was the high real part of the patch antenna input impedance. It was found that the quality of the impedance matching controls the tag's temperature-sensitivity: increasing the power transfer between the IC and antenna reduced the temperature sensitivity and vice versa. A choice was made to provide good impedance matching, as the use of dissipative distilled water would already reduce the attainable read ranges.
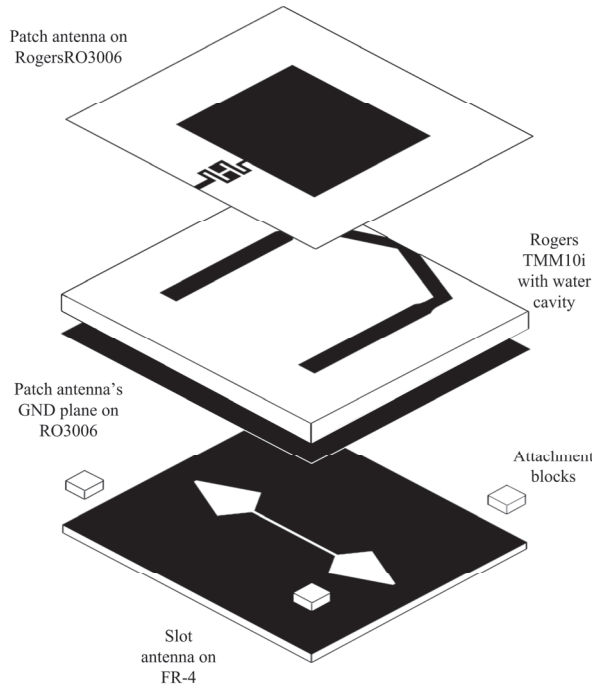

Fig. 12. Structure of the dual port temperature sensor tag [P3].
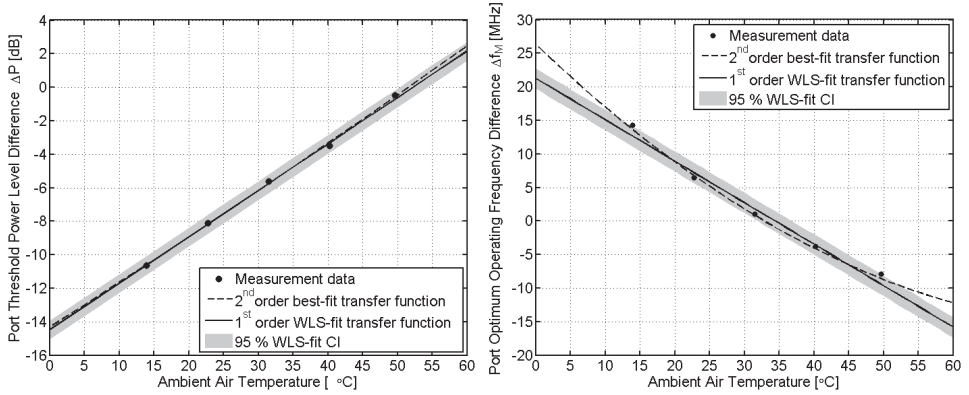
Fig. 13. Transfer functions of the dual port temperature sensor tag [P3].

The choice to use a slot antenna as the reference was due to the close proximity of the patch antenna's ground plane, which introduces additional self-capacitance. The inherent inductive input impedance of the slot antenna made the impedance matching less complicated and allowed relatively simple antenna geometry. An additional air gap was needed to reduce the coupling between the patch and slot antennas as well as to increase the slot antenna's radiation efficiency sufficiently. The mutual coupling between the ports plays an important role in the overall accuracy of the sensor tag, if the coupling is too great, the accuracy of the sensor decreases. In simulations, the coupling between the two ports was below -28 dB at the operation band of the sensor, which is sufficient to enable high sensor accuracy [P3].

The measured, normalized threshold power radiation patterns [84] of both tags in [P3] confirm that the reference port is also readable from the broadside direction of the patch, even though it is located behind the patch antenna's ground plane. The presence of the slot antenna also causes the patch antenna to be readable from its backside.

The temperature characterization performed on the sensor tag, showed that the threshold power of the patch-type tag changes with the temperature while the slot-type tag's threshold remains fairly stable. Transfer functions linking the relative differences in port threshold power levels (ΔP_{th}), at 940 MHz, and optimum operating frequencies (Δf_{opt}) with ambient temperature are listed in Table 6 and shown in Fig. 13.

Table 6. Measured sensor performance parameters [P3].

Readout method	Transfer function	Sensitivity	Accuracy	Resolution
ΔP_{th}	$0.28\,T - 14.49$	0.28 dB/°C	± 1.6 °C	0.36 °C (0.1 dB steps)
Δf_{opt}	$-0.62\,T + 21.3$	620 kHz/°C	± 2.4 °C	0.81 °C (0.5 MHz steps)

The maximal theoretical read range of the sensor varies between 3.4 to 4.6 meters in free space. However, the read range can be easily increased by utilizing a more sensitive RFID IC. For example RFID IC used in the design Higgs-2 has a power sensitivity of -14 dBm, while a newer Higgs-3 has a power sensitivity of -18 dBm.

The practical performance of the dual port temperature sensor tag was examined in three different environments, shown in Fig. 14. These environments are all electromagnetically different, with different amounts of external interference. The readings produced by the sensor tag were compared against a traditional digital thermocouple thermometer. In all test cases, the sensor tag produced readings comparable to the digital thermometer, see Table 7. Of the two readout methods studied, the port threshold level difference was found to produce temperature readings closer to the digital thermometer. The basement environment showed the largest deviations in the readings between the sensor tag and digital thermometer. This was due to the high level of reflections and multipath propagation inside the room with walls, floors and ceilings made out of steel reinforced concrete.

Table 7. Measured temperature levels in different environments [P3].

Environment	Thermocouple reading	Sensor tag reading (ΔP_{th})	Sensor tag reading (Δf_{opt})
Basement	(20.4 ± 1.1) ˚C	(17.6 ± 1.9) ˚C	(17.2 ± 2.6) ˚C
Office	(21.6 ± 1.1) ˚C	(21.8 ± 1.9) ˚C	(23.9 ± 2.6) ˚C
Outdoor	(27.5 ± 1.1) ˚C	(27.4 ± 1.9) ˚C	(27.8 ± 2.6) ˚C
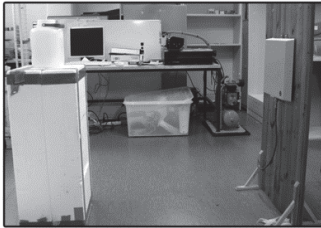
(a) (b) (c)

Fig. 14. Testing locations: (a) basement (b) office (c) outdoors [P3].

4. Inkjet-Printed UHF RFID tag antennas

In the concept of Internet of Things all the objects in the world would be uniquely identifiable, they would contain information that could be queried by mobile, hand held, or stationary reader devices. Some of these objects could communicate and share information between them, without the presence of specific reader units. As it was already noted in Section 1.1, UHF RFID is one of the technologies of today that could enable the Internet of Things.

However, many challenges related to the pervasive use of UHF RFID technology still exist [85]. Most of the challenges are related to system level issues, such a communication protocols and standardization. Issues regarding hardware level include the cost of tags and their integrability of tags to various everyday objects, which arises from the modern fabrication methods of tag antennas.

Photolithography is widely used to fabricate the RFID tag antennas of today, which are typically made out of copper or aluminum. Photolithography requires many steps such applying and developing the photoresist, etching, electroplating etc. Photolithography generates great amounts of wastage, leading to inefficient use of materials. Furthermore, the solvents used in the process are corrosive. This limits the types of substrates suitable for photolithography. To solve this problem, RFID tags are fabricated on polymer inlays, which are compatible with the photolithography process. After fabricating and embedding the tags into a polymer, an adhesive layer is applied on one of the outer sides of the polymer inlay. This allows the RFID label to be attached to various products. However, labeling products with RFID tags after they have left the production line causes extra costs and delays. This issue can be seen as one of the major obstacles in the way of the Internet of Things.

Additive, direct write fabrication methods, i.e. printed electronics, are capable of producing low cost tags directly on a wide variety of substrate materials. In printed electronics, circuits and components are fabricated using conductive inks by screen printing, flexography, gravure, offset lithography or inkjet-printing. These fabrication methods are considered to be additive as ink is selectively deposited onto substrate materials to form circuits and components. The additive nature of printed electronics, which results in low material wastage, is one of the reasons for its low cost. Another fact reducing the cost of fabricated components is that printable electronics allows the use of novel low cost substrate materials for electronics manufacturing, e.g. renewable materials such as wood and paper. Thus, the use of printable fabrication methods alleviates the challenges in the integrability of RFID tags directly into typical objects of everyday use as the need for troublesome tag labeling is removed.

4.1   Fundamentals of drop-on-demand inkjet-printing

Inkjet-printing is a form of direct writing technology for digitally controlled, non-impact, no-mask deposition of functional materials. Inkjet-based direct writing involves the formation and deposition of a sequence of droplets of liquid material, often called an ink or fluid. Two types of inkjet-printing methods exist: continuous and drop-on-demand (DOD). In the continuous method ink droplets are continuously formed and guided to place using electric fields, while in the DOD inkjet-printing droplets are formed only as they are needed [86]. Now on, DOD inkjet-printing is focused as it was the method of choice in the work presented in [P4-P7].

A DOD inkjet-printer, in Fig. 15-16, consists of an ink reservoir connected to print head and a platen that carries the printing substrate. Ink droplets are formed by the print head through thermal, piezoelectric, electrostatic or acoustic excitation. The most common method in order to form droplets is through electrically driven piezoelectric element inside the print head. In such excitation, the ink from the ink reservoir is poured into a cavity inside the print head. A droplet is ejected from the nozzle of the printed as external voltage pulse is applied over the piezoelectric material, typically lead zirconium titanate. The applied voltage causes a physical deformation in the piezoelectric material, which in turn generates a pressure wave inside the print head cavity and ejects the droplet. The volume of the droplet is covered by the volume of the print head and it can vary between 500 fl to 2 nl [86]. The platen, carrying the printing substrate, is located under the print head. The platen and print head can be moved by electric precision motors and thus lines can be printed on the substrate. The diameter of the landed droplet depends on several process parameters such as: ink viscosity, ink temperature, jetting voltages and frequency as well as the surface properties and temperature of the substrate material. After the features have been formed on the substrate the ink needs to be cured or sintered to make it solid (in case of dielectrics) or conductive (in inks with metallic content).
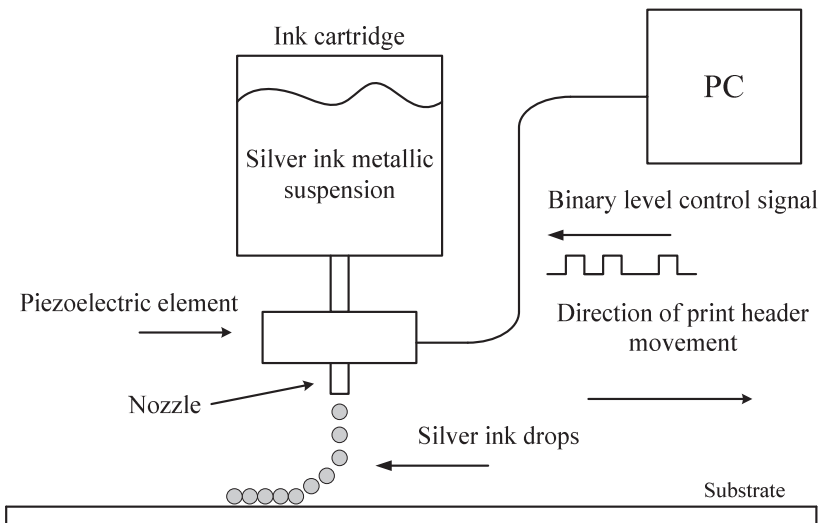

Fig. 15. Simplified schematic of a drop-on-demand inkjet-printer.
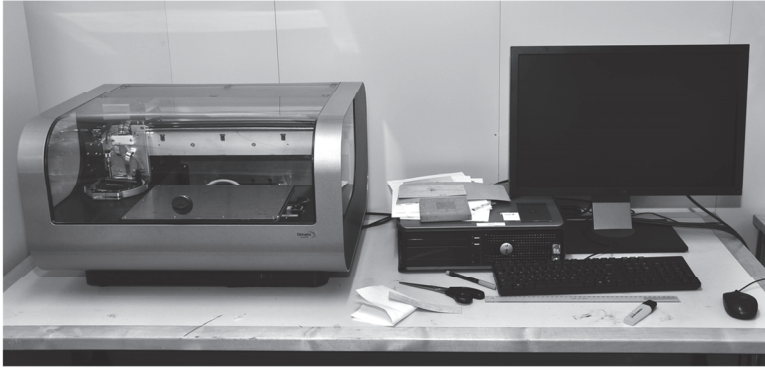
Fig. 16. Dimatix DMP-2800 a DOD inkjet-printer used to fabricate tag antenna samples in [P4,P6-P7].

Inks used in the inkjet-printing process can be of conductive, semi-conductive or dielectric nature. Inks utilized in inkjet-printing need to be low viscous liquid phase materials [86]. Typically, conductive inks are metallic nanoparticle suspensions consisting of nanoparticles of metals and solvents or conductive polymers. Metallic suspensions exhibit higher conductivities, but they are also more expensive than the conductive polymers. Due to their better conductivity, metallic suspensions are generally used over conductive polymers.

Typically, the metals used in the conductive inks are silver, copper or gold nanoparticles with 2-4 times higher resistivities than their bulk counterparts. Table 8 lists some of the common inkjet-printable metallic suspensions. Silver is preferred due its high conductivity and anti-oxidation properties [87]. The drawback of silver and gold is their price, which makes them less attractive to be used in mass production. Copper, on the other hand, is cheaper, but has lower conductivity and is easily oxidized. The use of tiny metallic nanoparticles is favored as it increases the stability of the suspension: small particles are less likely to sediment and clog the nozzles. In addition, using small particles with high surface to volume rations reduces the sintering temperatures [88].

In the sintering stage, the small nanosized metallic particles bond together to form a solid layer of metallization, see Fig. 17. Sintering is a relatively low temperature process; the melting point of bulk silver is around 960 ˚C, whereas the melting point of silver nanopar-
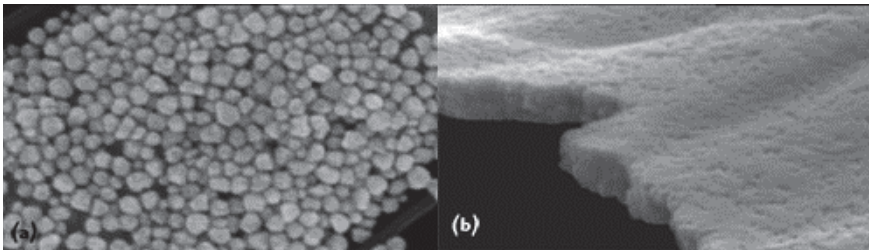

Fig. 17. Example of silver ink sintering: a) before sintering b) sintering at 180°C for 10 minutes. [114]

ticles is between 150 ˚C to 300 ˚C, depending on the particle diameter. The sintering temperature and time have an effect on the resistivity of the metallic layer: higher temperatures and longer exposure times lead to lower resistivity. The sintering can be done using traditional or convection ovens or by laser if shorter sintering times are required [89]. [90]

Table 8. Properties of typical conductive inks for inkjet-printers.

Ink	Particle size [nm]	Metal content [wt%]	Resistivity [μΩ·cm]	Skin depth at 900 MHz [μm]	Sintering conditions [˚C, min]
NPS-J (silver) [91]	12 nm	62-67	3	2.9	220, 60
NPS-JL (silver) [91]	7 nm	52-57	4-6	3.4 - 4.1	120-150, 60
CCI-300 (silver) [92]	Few nm	19-21	4-80	3.4 - 15.0	100-350, 60
NPG-J (gold) [91]	7 nm	50-55	12	5.8	250, 60

4.2 Inkjet-printing in UHF RFID tag antenna fabrication

Inkjet-printing UHF RFID tag antennas promises to bring to big benefits that can aid RFID technology to become more wide spread and eventually to enable the existence of Internet of Things. The biggest benefit of inkjet-technology is that it allows tag antennas, or in the future even the whole tag [93], to be printed directly on to products or product packages already at the production lines. The use of inkjet-printing allows tags to be printed on flexible or rigid, planar or even 3-D, smooth or rough surfaces. In addition, as the method is non-impact, non-corrosive and low temperature, it allows the utilization of sensitive and low cost substrate materials: for example, the use of ultra-low cost paper and wood is demonstrated in Section 4.4. Furthermore, new the use of a ceramic-polymer composite as a tag antenna substrate is validated in the same section.

Another benefit of inkjet-printing in tag antenna production is that it allows rapid prototyping with low cost. This is due to the fact that patterns formed by inkjet-printing are formed from digital images that can be switched in an instant to fabricate other designs. No masks are needed which also speeds up prototyping and enables low cost setup costs. In addition, inkjet-printing enables the fabrication of low cost application-specific tag antennas: these types of tags are designed to operate specifically on certain substrate, or on a certain sized or shaped object.

The main challenge related to inkjet-printed tags at the moment is the cost of conductive inks as noted before. However, the current development of conductive inks, suitable for inkjet-printing aims to bring low cost inks with higher conductivities. Development efforts are targeted toward the use of graphene and copper. These advancements suggest

that the cost of inkjet-printable inks should be dramatically lowered in the future. Nonetheless, inkjet-printed tags suffer also from a fundamental property of the fabrication method: an inherent property of inkjet-printed conductors is that their thickness is in the order of a few micrometers at most and that their conductivity is well below the bulk value of the metal particles. This creates challenges fabricating antennas with high efficiencies due to the power losses in the inkjet-printed conductors.

In general, power losses in arbitrary conductors can be calculated using the time-average power entering the conductor. Assuming an interface between a lossless medium and perfect conductor, with a cross-section S, where the field is incident from $z<0$ and propagates into the conductor at $z>0$, the time-average dissipated power becomes [94]

$$P_{av} = \frac{1}{2}\text{Re} \int_S \bar{E} \times \overline{H^*} \cdot \hat{z} \, ds = \frac{R_s}{2} \int_S |\bar{H}_t|^2 \, ds = \frac{R_s}{2} \int_S |\bar{J}_s|^2 \, ds, \qquad (30)$$

where $\bar{E}$ and $\bar{H}$ are the incident electric and magnetic field intensity vectors, H_t and J_s are the tangential magnetic and surface currents on the conductor, R_s stands for the sheet resistance $\left(\frac{\Omega}{\square}\right)$. The sheet resistance of a rectangular conductor, conducting direct current (DC), can be calculated using [95]

$$R_{S,DC} = \frac{1}{\sigma t}, \qquad (31)$$

where σ is the conductivity of the material and t is the thickness of the conducting layer. At DC, the whole cross-section of the conductor carries the current. However, once alternating current is driven through the conductor, the current flows mainly on the surface of the conductor due to the skin effect. At high frequencies, the electric field entering the conductor attenuates exponentially. Again if a x-polarized electric field is incident on a conductor with conductivity σ that occupies $z>0$, the electric field can be stated as [95]

$$\overline{E_x} = E_{x0}e^{-\alpha z}, \qquad (32)$$

This leads to exponentially decreasing current density within the conductor [95]

$$\bar{J}_x = \sigma E_{x0}e^{-\alpha z}, \qquad (33)$$

where E_{x0} is the magnitude of the electric field on the surface of the conductor and α is the attenuation constant, which in good conductors can be defined as $\alpha=\sqrt{\pi f \mu \sigma}$. The inverse of the attenuation constant is called *the skin depth* of the conductor δ, which describes the distance from the conductor's surface where the current density has dropped to $1/e$ from its initial magnitude. The total current flowing I through a conductor with a cross-sectional area S can be calculated by integrating the current density over the face $I = \int \bar{J}_x dS$. For a rectangular conductor with thickness t, width w and length L, the integration yields [95]

$$I = \int_{z=0}^{t} \int_{y=0}^{w} \sigma E_{x0}e^{-\alpha z} \, dydz = \frac{w\sigma E_{x0}(1-e^{-\alpha t})}{\alpha} = w\sigma E_{x0}\delta(1 - e^{-\alpha t}). \qquad (34)$$

The resistance of such rectangular conductor can be calculated by [95]

$$R = \frac{V}{I} = \frac{E_{x0}L}{w\sigma E_{x0}\delta(1-e^{-\alpha t})} = \frac{1}{\sigma\delta(1-e^{-t/\delta})}\frac{L}{w} = R_s\frac{L}{w}, \tag{35}$$

From Eq. (35) it is visible that is the conductor has low thickness compared to the skin depth of the conductor, the effective resistance and power losses of the line will increase. [96]

In Fig. 18, the sheet resistance of a non-magnetic conductor with 20 MS/m conductivity is plotted as a function of its thickness in terms of skin depths at 900 MHz (skin depth for such conductor at 900 MHz is 3.75 μm). The minimal sheet resistance of a given conductor can be calculated by $R_s=1/\sigma\delta$. Fig. 18 shows that once the thickness of the conductor is around five times the skin depth, the increased resistance due to skin effect is nearly removed. Therefore, to fabricate low loss conductors from a given conducting material, their thickness should be around four to five times the skin depth.

The abovementioned discussion about the power losses is valid for conductors with rectangular cross-sectional areas. The cross-sectional area of an inkjet-printed conductor is usually quite irregular and depends heavily on the printing process parameters [97]. Nonetheless, the effects of conductor thickness and conductivity are similar in inkjet-printed conductors as well.

Typically, the thickness of inkjet-printed conductors ranges between 0.5 μm to 2 μm per printed layer [97]. For example, in [P4] it was found that with the particular settings the silver ink metallization was around 1.4 μm per layer as shown in Fig. 18. The thickness of the conductor is affected by several process parameters such as, type of ink and substrate, substrate surface tension, printing resolution, drop volume, jetting waveform and the temperature of the substrate. The data in Table 8 shows that the skin depth of inkjet-printed conductors and especially their low loss thickness (5δ) are several times thicker than the thickness of a single layer of ink. This implies that to produce relative low loss inkjet-
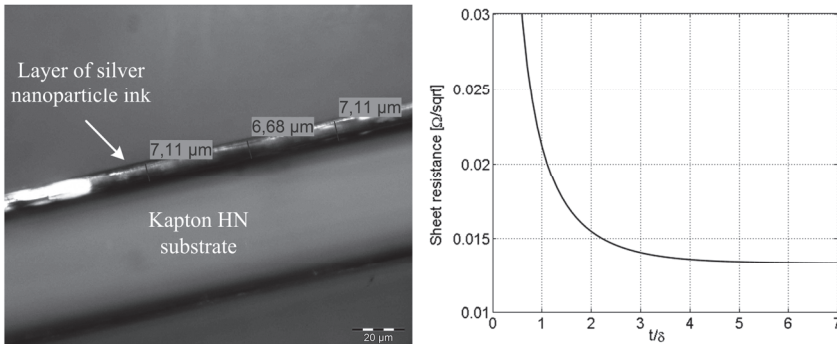

Fig. 18. On the left: Micrograph from a cross-section of an inkjet-printed conductor. On the right: Sheet resistance of a non-magnetic conductor (20 MS/m) at 900 MHz.

printed tag antennas they need to be printed using several ink layers [98].

The final challenge of inkjet-printed UHF RFID tag antennas is related to the mass production of tag antennas. The production speed of inkjet-printing, at least at the moment, is quite low compared to other methods of printed electronics, e.g. roll-to-roll gravure printing. This is due to the movement speed and nozzle count of print heads. At the moment, the movement speed of the print head is around 1 m/s. On the other hand, increasing the amount of nozzles depositing ink will lead to faster production. Moreover, sintering takes time, but advanced laser sintering could be used to reduce the required time.

4.3   Optimization techniques for improved cost-efficiency

This section presents work, which introduces a selective deposition method [P4] and a novel tag antenna structure [P5] to reduce the cost of inkjet-printed UHF RFID tag antennas, while maintaining sufficient read range performance. The cost reduction is done by minimizing the amount of ink needed to fabricate tag antenna structures.

4.3.1   Selective deposition of tag antennas

In order to reduce the amount ink required to fabricate high performance tags, a selective ink deposition method is presented in [P4]. The method relies on the identification of areas on the tag antenna, which exhibit high current density levels using an electromagnetic simulator. In the selective deposition, the antenna pattern is first printed fully using a single layer, then additional layers of conductive ink are added to the areas with high current density levels. In theory, most of the power dissipation occurs in these areas and the addition of ink to these areas should yield the biggest impacts on the antenna efficiency – thus improving the cost-performance ratio of the tag antenna.

In [P4], the selective deposition method was evaluated on the small dipole-type tag antenna geometry presented, later referred as the *test tag antenna*. Ansoft HFSS, a finite element based EM simulator was used to identify the areas with high current densities on the test tag antenna. The main challenge in the selective deposition of tag antennas is to identify the areas with sufficient current density levels, which justify the increase in ink thickness: too low level results in the inefficient use of ink, while selecting excessively high level leads to poor performance. The solution to this challenge in [P4] was to create several different deposition masks based on different current density levels. Three different masks were created, all based on different levels of surface current density. These masks add ink onto areas which exhibit 5, 10 and 40 times higher current density levels than the current density found in the center regions of the dipole arm ends. Furthermore, two masks were created for additional comparison. These masks are not based on any simulations, but on empirical knowledge. They add ink to the areas of the impedance matching network, as it exhibits the highest current density levels and to the dipole arms only. The masks used in [P4] are presented in Fig. 19.
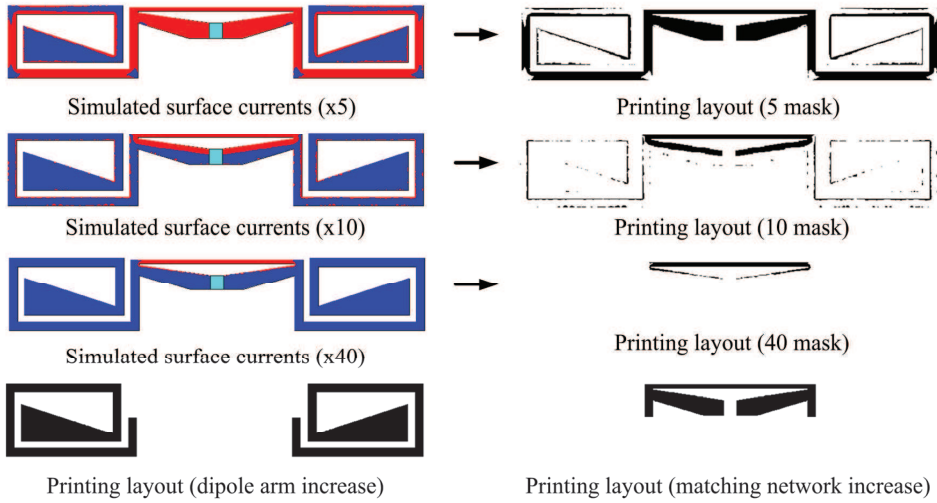
Fig. 19. Selective deposition masks used in [P4], the red color indicates high surface current density levels that exceed the given threshold indicated within the brackets.

The effectiveness of the selective deposition was compared against a method, where the full antenna pattern was printed using multiple layers or ink. Samples of tag antennas fabricated using selective and full deposition were printed using a Dimatix DMP-2800 inkjet-printer with 10 pl nozzle heads on to 50 μm thick Kapton® HN polyimide substrate. Harima NPS-JL was used as the conductive ink. The printing resolution was set to 282 dpi as it was found optimal for the combination of Kapton® HN and NPS-JL. A passive Higgs-3 RFID IC was attached to the inkjet-printed tag antennas using a conductive epoxy resin. The tag antennas with full layers were printed using one to five layers of ink, while the selective deposition, on top of the single full layer, was done using one to four layers. The antennas were sintered at 200 ˚C for 40 minutes between each printed layer.

Cross-sectional images, shown in Fig. 18, of the inkjet-printed samples in [P4] revealed that the mean thickness of a single layer of ink was around 1.4 μm close to the impedance matching network, which is about a third of the skin depth at 900 MHz. At five printed layers, the silver layer was around 1.7 times the skin depth. However, it should be noted that the thickness of the conductive layer may have large variations from the measured values in different parts of the tag antenna and depending on the printing direction.

Fig. 20 presents the measured theoretical read range of the tag's equipped with the test tag antenna printed using selective deposition masks as well as with full layers. The dots represent measured values, the solid lines are polynomial fits of the measured data and the dashed lines illustrate the estimated increase in the tag's read range if more ink would be added using the particular mask.

The results show that the tag samples with tag antennas printed using full layers had the highest read range after printing five layers in total. The *5 mask* selective deposition is the
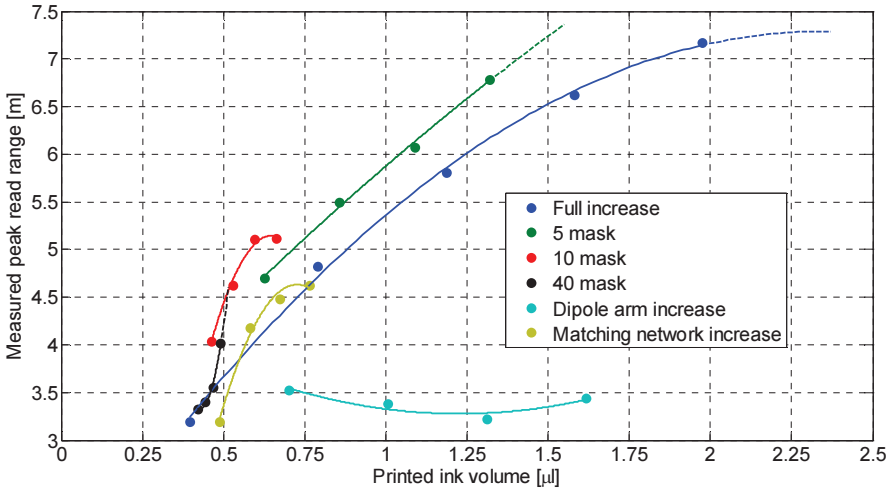
Fig. 20. Measured peak read range of the samples as a function of ink consumption [P4].

highest performing selective deposition mask. The estimated trend of the read range performance of *5 mask* shows that it could match the read range of the full increase case is more layers would be added. All samples printed with the *5, 10* or *40* selective deposition masks exhibit greater peak range to ink consumption ratios, i.e. cost-performance ratios, than samples printed with multiple full antenna layers. The highest cost-performance ratio is obtained by using the *10 mask* selective deposition as it produces relatively long read range with low ink consumption. The effectiveness of the selective deposition is validated by examining the results obtained from the samples printed using the matching network and dipole arm increase masks. Increasing the ink layer on the matching layer is less efficient than *10 mask* and *40 mask* increases. The worst performing selective deposition mask is the dipole arm increase.

Table 9. Calculated reduction in total ink consumption at different performance criteria [P4].

Performance criteria	Selected deposition mask	Possible savings in ink consumption vs. full increase
7 m	5 mask (projected)	22.1 %
6 m	5 mask	31.1 %
5 m	10 mask	49.8 %
4 m	10 mask	41.6 %

The measurement results from Fig. 20 allow the determination of the amount of possible ink savings due to the use of selective deposition. The amount of ink savings can be calculated against the full increase assuming different performance criteria for the tag read range, as shown in Table 9. The assumption of different performance criteria is justified since not all applications require the maximal read range from a given tag design. Table 9

shows that significant reductions in the total amount of ink are available by utilizing the selective deposition. This reduction in the ink consumption can be related directly to the cost of a tag antenna.

An alternative method for reducing ink consumption is presented in [99]. In this method, the tag antenna is divided into grids and only the edges of the grids are printed. The authors have reported reductions of over 50 % in the antenna surfaces areas. The drawback of such gridding compared with the selective deposition is that it reduces antenna efficiency and alters the input impedance of the antenna. These changes increase as the antenna is divided into smaller and smaller grids. Eventually the antenna's radiation efficiency and impedance matching to the load, e.g. RFID IC, are degraded to a point, which do not enable reliable tag operation.

4.3.2 Narrow-line UHF RFID tag antennas

In addition to the selective deposition method, novel tag antenna structures can be utilized to minimize the consumption of conductive inks. One example of such tag antenna's, called the narrow-line tag antenna is presented in [P5]. The design methodology was to develop a dipole-type tag antenna for UHF RFID systems that utilizes the fine line printing capabilities of inkjet-printers. Commonly, one of the design aspects of UHF RFID tag antennas is to minimize their physical size. In the case of the narrow line tag, an alternative approach was used. The overall size of the tag antenna was kept fairly large, to offer good performance, while minimizing the widths of the dipole arms to reduce its surface area and thus ink consumption. The small line widths and surface area also allow for extremely fast production time by inkjet-printing.

The narrow-line tag antenna, depicted in Fig. 21 is roughly half-wave length long. The physical foot print of the antenna was slightly reduced by folding the dipole arms from
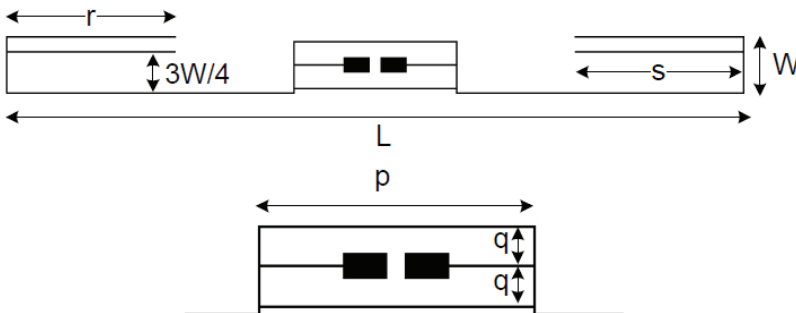
DIMENSIONAL PARAMETERS FOR THE TAG ANTENNAS

w [µm]	p [mm	q [mm]	r [mm]	s [mm]
50	19.6	2.8	21.3	20.0
125	21.9	2.2	16.5	23.9
200	21.9	2.8	22.8	22.8

Fig. 21. Narrow-line tag antenna geometry and key dimensions [P5].

their ends. The overall dimensions of the tag antenna are L=100 mm and W=7.6 mm. The dipole arms were fabricated with three different line widths (w): 50 μm, 125 μm and 200 μm. The arm width affects the tag antenna's input impedance and thus each width needed optimizations in to the tag antenna's key dimensions. The optimization was done using Ansys HFSS 12. In the optimization, the antenna and impedance matching network (double T-matching network [100]) dimensions were tuned to provide good impedance matching to the input impedance of the RFID IC of choice, Higgs-3. Reducing the arm width increases the tag antenna's input resistance and inductance, making the complex-conjugate matching challenging. This is especially apparent in the case where the arms were 50 μm wide as only 70 % of the simulated power available from the antenna is transferred to the IC.

The narrow-line tag antennas were fabricated using ITI XY MDS 2.0 inkjet-printer. The conductive ink was the NPS-J silver nanoparticle ink and it was deposited on a 50 μm thick Kapton HN polyimide film using 600 dpi as the resolution. Samples with all three different arm widths were printed using one to four ink layers and sintered after applying the final conductive layer at 200 ˚C for 60 minutes.

The measured theoretical read ranges of the inkjet-printed narrow-line tag antenna samples are presented in Fig. 22. The read range levels behave as excepted: thicker lines and conductive layers reduce the amount of power losses in the antenna and enable longer read ranges. However, the long distances of the read ranges are very surprising. Samples with 50 μm arm width exhibit peak read ranges from one meter to 4 meters. The peak
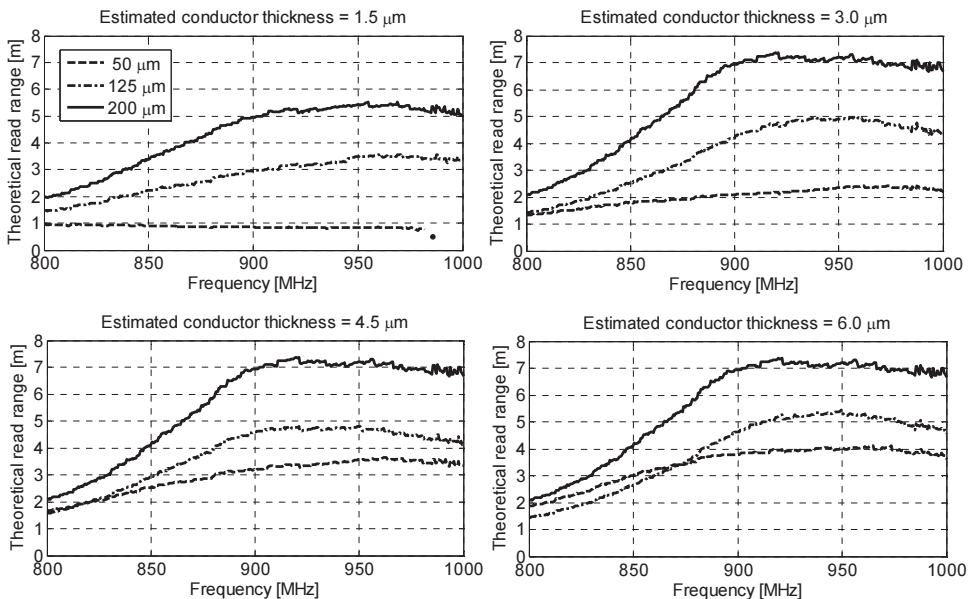

Fig. 22. Measured theoretical read ranges of each narrow-line arm width and conductor thickness [P5].

read range of samples with 125 μm arm width ranged from 3.5 to 5.1 meters. Narrow-line tags with 200 μm arm width were readable from distances between 5.1 to 7.2 meters. Interestingly, the read range performance of the 200 μm arm width samples was already saturated after two layers of NPS-J silver nanoparticle ink.

A read range comparison was performed in [P5] between a tag equipped with the inkjet-printed narrow-line tag (200 μm arm width, 3 layers of ink) and a high performance commercial copper-made dipole-type tag ALN-9640. Both tags are equipped with a passive Higgs-3 RFID IC. The peak read range of the ALN-9640 is slightly over three meters longer than the peak read range of tag with the inkjet-printed narrow-line tag antenna. However, at the U.S. band the read range difference is less than one meter. The performance of the inkjet-printed narrow-line tag antenna is exceptional taking into account that the ALN-9640 is made out of copper and that the narrow-line tag requires 83% less conductor surface area. Assuming that both antennas would be inkjet-printed, the narrow-line tag antenna would be almost five times cheaper in terms of ink costs and faster to fabricate.

The results in [P6] show that high performance inkjet-printed tag antennas can be designed with extremely narrow line width and low conductor thickness. The good read range performance of the inkjet-printed narrow-line tags was also verified in practical applications, once attached to different objects [101].

4.4 Inkjet-printed tag antennas on novel antenna substrate materials

This section presents work, where inkjet-printing has been used to form tag antennas directly on novel antenna substrate materials, which would not tolerate the traditional corrosive fabrication methods or enable novel tag antenna implementations. The demonstrated materials are birch veneer [P6], a ceramic-polymer composite [P7], ordinary paper and cardboard. These materials are all low-cost, but challenging as substrate materials for inkjet-printing. Utilization of these materials expands the applicability of UHF RFID technology significantly and provides further advancements toward the Internet of Things.

4.4.1 Birch veneer and plywood-embedded tag antennas

Plywood-based products are found everywhere. It is widely used as a construction material of houses, furniture, product packages and boxes. It is estimated that the global plywood market will reach 75.9 million cubic meters by 2015 [102]. Identifying and tracking all these products of plywood, individually using embedded passive UHF RFID technology, could bring several benefits to our everyday lives.

For example, in case of product defects, the origins of the product are easily discoverable. Similarly, product counterfeiting can be avoided by embedding the tag in to the product

itself: as the tag is embedded inside the plywood, product tampering is extremely challenging. In addition, embedding "dumb" wood with smart RFID labels, could enable the wide spread use of smart furniture and smart surfaces [103] [104]. For the manufacturers of the wood-based products, embedding the tags into the products could help keeping track of stock levels and allow the products to be tracked throughout the whole supply chain automatically at the item level.

However, embedding plywood with typical passive UHF RFID tags is rather difficult. Plywood is made out of thin sheets of wood veneer that is bonded together with adjacent plies having their grain at right angles to each other [105]. The wood veneer itself causes major challenges to the implementation of embedded UHF RFID tags. Wood does not withstand high temperatures or corrosive chemicals. Traditional lithography directly on wooden surfaces to create the antenna pattern is therefore not an option. The use of UHF RFID tags in polymer-based inlays is also impossible due to the popping of the plywood: The adhesives used in the plywood manufacturing process do not offer sufficient adhesion to such polymeric surfaces. Moreover, the thickness of such tags is often too great to allow them to be embedded inside plywood.

A novel solution this problem was proposed in [P6], where for the first time, tag antennas where inkjet-printed directly on to pure, non-coated, 0.4 mm thick birch veneer. It was found that the conductive silver nanoparticle ink was compatible with the adhesives used in the veneer bonding process and the plywood did not pop. Furthermore, the extremely thin thickness of the inkjet-printed tag antennas facilitated the successful embedding process. The RFID IC is the thickest component in the tag, approximately 100 to 200 μm in height. However, the foot print of the IC and its package are small enough to prevent any popping to take place.

The grain of the wood plays an important role in the tag implementation. It was found that tags printed along the grain showed higher read ranges than the ones printed against the grain. This finding is explained by the fact that by depositing ink in the direction of the grain leads to thicker conductive surfaces. Moreover, it was found that to maximize the tag antenna performance and process throughput of functional antennas, most of the tag antenna geometry should lie on one axis (in the direction of the grain) – to align the antenna currents with the thicker ink traces. This design aspect was named as the *one axis design rule*, which allows the fabrication of high performance tag antenna designs on wooden surfaces.

Two different tag antenna designs, based on the *one axis design rule*, were developed for birch wood veneer in [P6], these are presented in Fig. 23. The first design is called *a wide band tag antenna* as it was designed to exhibit a wide operation band. The second tag design, called c*ompact tag antenna*, was designed to occupy less space with the cost of a more narrow operation band. The key dimensions as well as the simulated power transmission coefficients and realized gains are listed in [P6]. Although, the antennas were
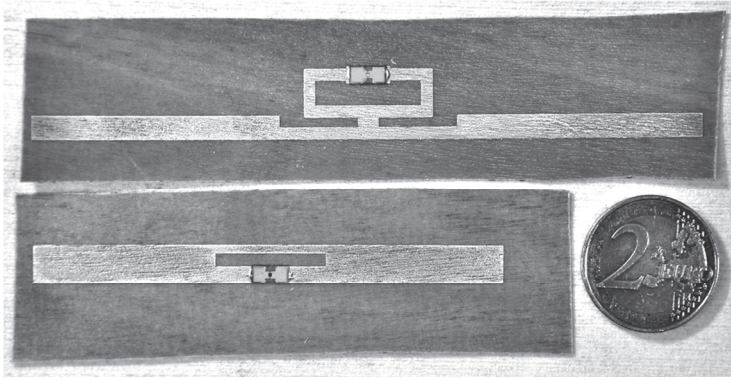
Fig. 23. Picture of directly inkjet-printed UHF RFID tag antennas on birch veneer. On top: wide band tag antenna. On bottom: compact tag antenna [P6].

printed on birch veneer, in their end application the veneers containing the antennas will be embedded inside plywood. Therefore tag antennas were designed explicitly for birch veneer substrate and their operation characteristics were optimized using HFSS EM simulator while embedded inside 2 mm thick plywood.

The inkjet-printing process of tag antennas on pure, non-coated, birch veneer involves the use of multiple ink layers at right angles to each other. This is done to fill the wood grain with ink to ensure good conductivity. The inkjet-printing process is described in detail in [P6]. In the final assembly of the tags, passive Higgs-3 RFID ICs were attached to the tag antennas using conductive epoxy resin. Both tags were later embedded inside a 2mm thick plywood board using a pressure of 10 bar for 300 seconds at 140 ˚C. The wide band tag was bonded using a wet adhesive, while the compact tag was bonded using dry sheet glue. This was done to validate that both adhesives can adhere to the silver ink layer to prevent the popping of the plywood.

Fig. 24 presents the measured threshold power levels and theoretical read ranges of both tag antenna designs while on the birch veneer substrate and while embedded inside 2 mm thick plywood boards. On the veneer, the wide band tag is readable from distances over 7.8 meters throughout the whole global UHF RFID band (860 MHz to 960 MHz) while the compact tag is readable from over 3 meters on the same band.

Results show that once embedded, the operation bands of both tags have shifted toward lower frequencies due to the material loading effects. This effect highlights the need for a wide band or robust tag antenna designs as the electrical properties of plywood are heavily dependent on the temperature and humidity [106]- [107]. If a narrow band antenna is used, the tag's readability can severely degrade at certain environmental conditions due to the changes of wood properties that modify the input impedance and radiation efficiency of the antenna. The peak read ranges of the plywood-embedded wide band tag and compact tag are 10.3 meters and 7.9 meters correspondingly. Increasing the plywood layer thickness around the tags will reduce their read ranges due to added signal attenuation. In
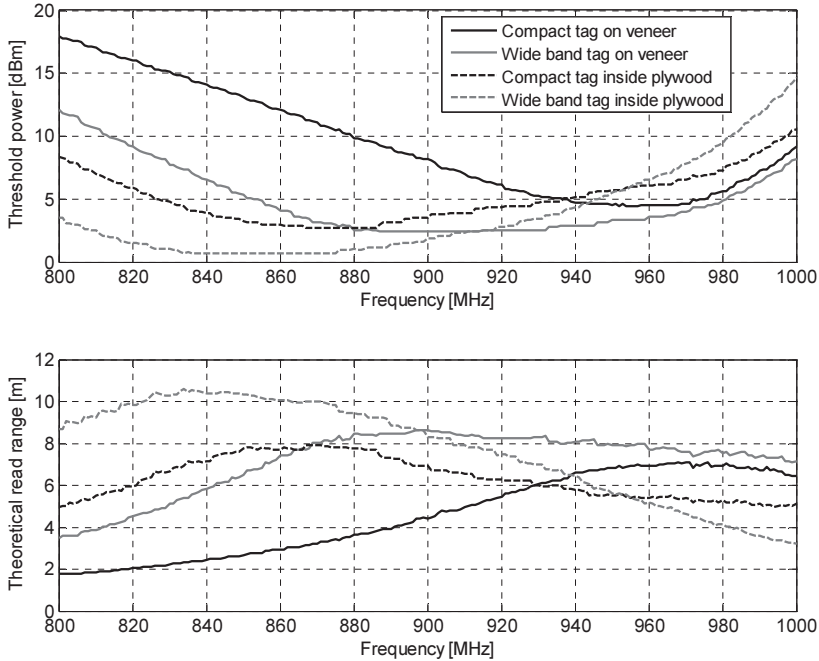
Fig. 24. Measured threshold power levels and theoretical read ranges of birch veneer and plywood-embedded tags [P6].

addition, it was found that the bandwidth of the compact tag is increased, while the bandwidth of the wide band tag is decreased as more plywood is added around the tags. The tag antenna radiation patterns were also affected by the added plywood, the omnidirectionality of the dipole antennas was lost in some cases, especially if the tags were placed asymmetrically within the plywood.

In conclusion, it was shown in [P6] that high performance passive UHF RFID tags are inkjet-printable directly on to veneer and embeddable into plywood. The performances of the tags are more than sufficient for the requirements of the plywood industry and for the end users of plywood-made products: tags are readable from a few meters away even when stacked in tall piles of plywood or embedded inside thick layers of plywood.

4.4.2 Ceramic-polymer composite

Novel composite materials consisting of a base polymer doped with high permittivity ceramics enable significant antenna miniaturization as well as on-metal operation. In [P7], the use of PDMS-BaTiO$_3$ ceramic-polymer composite was demonstrated as a flexible high permittivity substrate for an electrically small inkjet-printed tag antenna. Polydimethylsiloxane (PDMS) [108] is a most widely used type of a silicon based organic polymer, belonging to a group of siloxanes. PDMS material has high thermal stability, low surface tension, and bulk viscosity. Moreover, PDMS has extremely low conductivity, making it a low loss antenna substrate material. It is transparent in nature, durable at
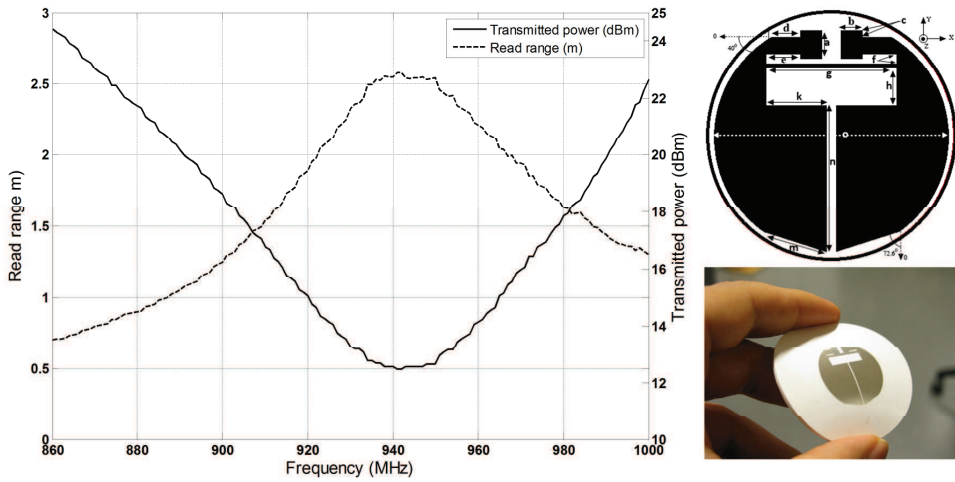
Fig. 25. On the left: measured threshold power level and theoretical read range of the inkjet-printed tag equipped with a Higgs-3 RFID IC on the composite substrate. On the right: tag antenna layout and picture of the inkjet-printed sample. [P7]

high temperatures, and hydrophobic. In elastomeric form PDMS is suitable for flexible substrates. Barium Titanate (BaTiO$_3$) is a high permittivity ferroelectric ceramic, usually available in powder form. Its permittivity depends on several factors, such as grain size, shape and size of the crystals, impurities, and on other processing techniques. Typically, the relative permittivity of BaTIO$_3$ ranges between ε_r=2000...4500 [109].

The composite can be doped with varying volume based ratios of BaTIO$_3$ to control the permittivity and losses of the composite. In [P7] the PDMS was doped using 20 %wt of BaTIO$_3$ with a mean grain size of 120 nm. It was estimated that the relative permittivity of the composite was around ε_r=15 at the global UHF RFID band. A small circular dipole tag antenna was designed for the composite, presented in Fig. 25. The diameter of the tag antenna is 26.5 mm (~0.08λ), more detailed dimensions are found in [P7].The tag antenna was inkjet-printed on the composite using Dimatix DMP-2800 printer with NPS-JL silver nanoparticle ink. The drop volume was 10 pl and the optimal printing resolution was found to be 847 dpi (30 μm drop spacing). The printing was done as follows: first two layers of silver nanoparticle ink was deposited, this was followed by a sintering stage in 170 ˚C for 40 minutes, after sintering two more layers were added and sintered one more time. Multiple layers of ink were needed to guarantee high conductivity as the high surface energy of the composite caused uneven ink distribution. After printing, the tag antenna was equipped with a Higgs-3 passive UHF RFID IC using conductive epoxy resin.

The measured threshold power level, from a distance of 45 cm, and theoretical read range of the circular tag antenna on the composite is shown in Fig. 25. The tag is operating at the global UHF RFID band. Its peak theoretical in free space read range is around 2.5 meters at 940 MHz. The optimal operating frequency could be tuned to the European or U.S. UHF RFID bands by adjusting the dimensions of the tag antenna's impedance

matching network. The finished tag could be shielded by an additional superstrate layer of PDMS to protect the IC and the inkjet-printed antenna. In a such configuration, he developed tag could be used as a robust, flexible UHF RFID label for small, possibly even metallic objects that is able to endure harsh environmental conditions.

4.4.3 Paper and cardboard

Integrating passive UHF RFID tags directly into paper and cardboard made products is also a challenge for the more traditional corrosive tag antenna fabrication methods. At the moment, the most feasible way of labeling books, magazines and cardboard boxes is to equip them with tags on a sticker. Such process is time consuming and generates extra costs. The best option would be to label the products while they are being fabricated.

A solution to this is also brought by the fabrication methods of printable electronics. Tag antennas can be printed on the products while they are on the production-line using silk screen printing, gravure printing or inkjet-printing. In fact, the same machinery used to print the patterns, e.g. text and logos, on the paper-based products could be used to add the conductive ink or paste to form the tag antenna. Only the automated attachment of the RFID IC would require additional machinery. The additional benefit is that paper is an ultra-low cost, renewable and environmentally friendly antenna substrate material. Thus, paper could be used in some applications as a substrate material for the sticker-type UHF RFID tags instead of more high cost polymers.

The use of silk screen printing and inkjet-printing has been demonstrated successfully on paper-based substrates for UHF RFID tag antenna fabrication [110] [111]. A major challenge, especially with inkjet-printing on paper-based materials is the absorption of ink. Paper can be coated to provide a fully hydrophobic surface for inks, as in [111]. However, tag antenna inkjet-printing can be done on water-absorbing paper as well [112].
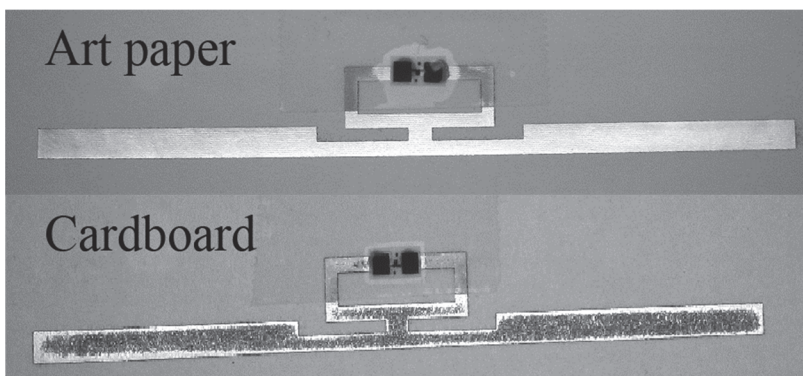

Fig. 26. Inkjet-printed wide band tag antennas on fine quality art paper (top) and on regular packaging grade cardboard (bottom).
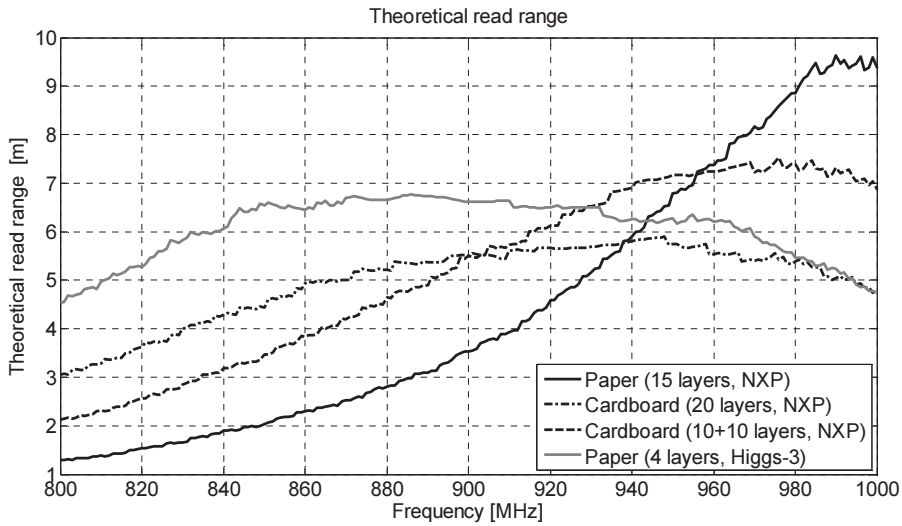
Fig. 27. Measured theoretical read ranges of the inkjet-printed wide band tag on water-absorbing paper and cardboard.

Fig. 27 presents the measured theoretical read ranges of an inkjet-printed wide band tag, layout presented in Section 4.4.1, on water-absorbing paper and cardboard. The paper substrate was a coated fine quality art 100 g/m^2 paper. Although the paper had a coating it was highly water-absorbing. The art paper provides a cheaper alternative to fully hydrophobic paper qualities. The cardboard was a UV-coated water-absorbing quality, used in typical product packages. The tags were printed using DMP-2800 printer with NPS-JL silver nanoparticle ink at 423 dpi resolution. The drop volume was 10 pl. The amount of ink layers and the RFID IC attached to the antenna are indicated in the figure legends. The ICs used, Higgs-3 and NXP GiL2 [113], have similar power sensitivity levels (-18 dBm), but slightly different input impedances. The notation '10+10' layers in the figure legend indicates that the tag antenna was printed using 10 ink layers, followed by additional 10 layers. Sintering at 150 ˚C for 60 minutes was done after printing ten and twenty layers.

The results show that it is possible to print high performance passive UHF RFID tag antennas on pure, water-absorbing, paper-based materials [112]. Even with four layers of ink, the tag antenna exhibits a read range of over six meters throughout the whole global UHF RFID band. Using 15 layers of ink, the peak read range is nearly ten meters. On cardboard the performance is slightly lower and more ink is required for high performance due to greater absorption of ink by the cardboard. It should be noted that the abovementioned study did not focus on determining the minimum amount of ink required to produce a fully operational tag antenna. Thus, the amount of ink layers could be decreased with the compromise of decreasing the tag peak read range.

5. Conclusions and final remarks

In the future, our lives will be surrounded by pervasive computing environments, where all the information will be available to everyone by everything. At the core of such ambient intelligence are ubiquitously deployed sensors, which gather information about their environment and forward it to the users, and smart objects, which are uniquely identifiable, traceable and in some cases able to communicate with each other. Radio frequency identification technology, along with other technologies offering wireless low-power communication, is seen as one of the enabling technologies for such ubiquitous sensing and Internet of Things. Passive UHF RFID technology, especially, is capable of offering low-cost, integral labels that are hidden from their users and able to prove automated long range identification and tracking of various things. In addition, passive UHF RFID can be used as one of the implementation methods of completely passive and wireless low-cost sensor devices for ubiquitous sensing applications. Although, passive UHF RFID provides many capabilities and solutions to pervasive computing applications, the true realization of pervasive computing requires a combination of different technologies, such as HF RFID and wireless sensor networks.

The main challenges related to the abovementioned capabilities of passive UHF RFID are the integrability and cost of the tags. In order for the technology to become ubiquitous the tag fabrication and integration costs should be as low as possible. In addition, a major obstacle for the current fabrication methods for RFID tags is that the products are labeled manually after leaving the production lines. Finally, the implementation of sensory functions to completely passive RFID tags is challenging. The work presented in this thesis was especially designed to provide solutions to these challenges.

First, it was shown that passive wireless sensor tags can be implemented using passive UHF RFID technology by the ingenious use of material properties. The implementation method of the sensor tags presented in this thesis is the lowest cost solution available at the moment: tag antenna based sensing, which removes the need for any discrete sensor components or specific ICs with sensory functions. The studies performed on the sensor tags in this thesis proved, for the first time, that such low-cost sensor tags able to provide sufficient levels of accuracy in many applications. Tag antenna based sensing allows the monitoring of various parameters, such as the temperature, humidity, air quality and strain. The sensor tags are based on the ISO-18000-C standard, which eases the integration and enables these special purpose tags to be operated by low-cost reader units. In the future, as ultra low-cost chipless RFID technology becomes more standardized, the same sensor development methods, presented in this thesis, can be used to create chipless sensor tags. The use of low cost passive sensor tags utilizing tag antenna based sensing does not come without challenges. The main issue is that the surrounding environment can have significant effects on the accuracy and readability of such tags. These issues can be

minimized by careful tag design, local on-site calibration procedures and by the further development of more robust wireless sensor data readout methods and antenna topologies. One such method, the dual port sensing concept, was presented in this thesis. In addition, local regulations concerning the bandwidth and allowed transmit power levels place limitations on the dynamic range of sensor tags utilizing tag antenna based sensing. This could be changed in the future, if the future potential of these tags can be validated.

The second part of this thesis was focused on inkjet-printed tag antennas. Inkjet-printing, along with other printable electronics fabrication methods, promises to ease the tag integration to the products already at the production lines. These methods, could be used, for example, to add the tag directly on or in to the product packages, removing the time-consuming and manual tag attachment process that is done nowadays. Inkjet-technology is especially interesting as a tag fabrication method since it can be used to manufacture application-specific tag antennas quickly and with low cost on to novel rigid, flexible and sensitive substrate materials. Also, in the future, the development of printable materials could allow the whole tag to be inkjet-printed. The major problem nowadays is the cost of the conductive inks used to create the tag antennas. This thesis has provided solutions to lower these costs. First, a selective deposition method was presented, which was shown to as much as half the amount of ink required to fabricate a high performance tag antenna. Secondly, a special tag antenna design made out of extremely narrow lines was presented. The tag antenna was shown to exhibit long read ranges, while requiring significantly less conductor surface area than a typical commercial tag antenna. These results show that narrow lines and low conductor thicknesses are able to provide low cost tag antennas, which is against the common conception. This thesis also showed that inkjet-printing can be used to create high performance tag antennas directly on to ultra low-cost and environmentally friendly substrate materials such as birch veneer, paper and cardboard. As we known, countless items are made out of paper and wood based materials, equipping these items with embedded passive UHF RFID tags could truly aid in the realization of the Internet of Things.

All in all, the innovative use of both novel and traditional engineering materials that enable passive sensor integration into passive UHF RFID tag antennas and the development of cost-efficient inkjet-printed tag antennas embeddable directly to various objects are key factors in the realization of concepts such as the Internet of Things and ubiquitous sensing that will revolutionize the way of life in the future.

References

[1] M. Weiser, "The computer for the 21st Century," *Scientific American,* vol. 265, no. 3, pp. 66-75, 1991.

[2] M. Satyanarayanan, "Pervasive computing: vision and challenges," *IEEE Personal Communications,* vol. 8, no. 4, pp. 10-17, 2001.

[3] M. Sánchez, M. Mateos, J. Fraile and D. Pizarro, "Touch Me: A New and Easier Way for Accessibility Using Smartphones and NFC," in *Advances in Intelligent and Soft Computing: Highlights on Practical Applications of Agents and Multi-Agent Systems*, Berlin / Heidelberg, Springer, 2012, pp. 307-314.

[4] B. Braiker, "Google Project Glass: a new way to see the world," 5 April 2012. [Online]. Available: http://www.guardian.co.uk/world/us-news-blog/2012/apr/05/google. [Accessed 8 May 2012].

[5] D. Estrin, D. Culle, K. Pister and G. Sukhatme, "Connecting the Physical World with Pervasive Networks," *IEEE Pervasive Computing,* vol. 1, no. 1, pp. 59-69, 2002.

[6] D. Saha and A. Mukherjee, "Pervasive computing: a paradigm for the 21st century," *Computer,* vol. 36, no. 3, pp. 25-31, 2003.

[7] ITU-T, "Technology Watch Briefing Report Series, No. 4: Ubiquitous Sensor Networks (USN)," ITU-T, 2008.

[8] ITU-T, "ITU Internet Reports: The Internet of Things," ITU-T, 2005.

[9] G. Kortuem, F. Kawsar, D. Fitton and V. Sundramoorthy, "Smart objects as building blocks for the Internet of things," *IEEE Internet Computing,* vol. 14, no. 1, pp. 44-51, 2010.

[10] M. Kumar, S. Das and A. Zomaya, "Pervasive Computing: Enabling Technologies and Challenges," in *Handbook of Nature-Inspired and Innovative Computing*, Springer US, 2006, pp. 613-631.

[11] V. Stanford, "Pervasive computing goes the last hundred feet with RFID systems," *IEEE Pervasive Computing,* vol. 2, no. 2, pp. 9-14, 2003.

[12] Auto-ID Labs, "Architecture Development for Sensor Integration in the EPCglobal Network," 2007.

[13] R. Want, "Enabling ubiquitous sensing with RFID," *Computer,* vol. 37, no. 4, pp. 84-86, 2004.

[14] D. Ranasinghe, K. Leong, M. Ng, D. Engels and P. Cole, "A Distributed Architecture for a Ubiquitous RFID Sensing Network," *Proceedings of the 2005 International Conference on Intelligent Sensors, Sensor Networks and Information Processing,* pp. 7-12, 2005.

[15] L. Zhang and Z. Wang, "Integration of RFID into Wireless Sensor Networks: Architectures, Opportunities and Challenging Problems," *Fifth International Conference on Grid and Cooperative Computing Workshops,* pp. 463-469, 2006.

[16] J. S., T. Sanchez Lopez and D. K., "The EPC Sensor Network for RFID and WSN Integration Infrastructure," *Fifth Annual IEEE International Conference on Pervasive Computing and Communications Workshops,* pp. 618-621, 2007.

[17] IEEE, "IEEE Standard for Smart Transducer Interface for Sensors and Actuators-- Transducers to Radio Frequency Identification (RFID) Systems Communication Protocols and Transducer Electronic Data Sheet Formats," IEEE, 2010.

[18] K. Finkenzeller, RFID Handbook: Fudamentals and Applications in Contactless Smart Cards and Identification, West Sussex: John Wiley & Sons Ltd., 2003.

[19] R. Das and P. Harrop, "RFID Forecasts, Players and Opportunities 2011-2021," IDTechEx, 2011.

[20] I. O. f. Standardization, "ISO-18000," 2011. [Online]. Available: www.iso.org. [Accessed 5 June 2012].

[21] T. Shiraishi, N. Komuro, H. Ueda, H. Kasai and T. Tsuboi, "Indoor Location Estimation Technique using UHF band RFID," *International Conference on Information Networking,* pp. 1-5, 2008.

[22] T. Kellomaki, T. Björninen, L. Ukkonen and L. Sydänheimo, "Shirt collar tag for wearable UHF RFID systems," *Proceedings of the Fourth European Conference on Antennas and Propagation,* pp. 1-5, 2010.

[23] G. Marrocco, "RFID Antennas for the UHF Remote Monitoring of Human Subjects," *IEEE Transactions on Antennas and Propagation,* vol. 55, no. 6, pp. 1862-1870, 2007.

[24] D. Dobkin, The RF in RFID: Passive UHF RFID in Practice, Burlington, MA: Elsevier Inc., 2008.

[25] P. Nemeth, L. Toth and T. Hartvanyi, "Adopting RFID in supply chains," *2006 IEEE International Conference on Mechatronics,* pp. 263-266, 2006.

[26] M. Attaran, "RFID: an enabler of supply chain operations," *Supply Chain Management: An International Journal,* vol. 12, no. 4, pp. 249 - 257, 2007.

[27] W. He, Y. Huang and W. Sun, "A UHF and HF RFID Integration System for Access Control," *Progress In Electromagnetics Research Symposium Proceedings,* pp. 111-114, 2010.

[28] U. Karthaus and M. Fischer, "Fully integrated passive UHF RFID transponder IC with 16.7-µW minimum RF input power," *IEEE Journal of Solid-State Circuits,* vol. 38, no. 10, pp. 1602- 1608, 2003.

[29] S. Srikant and R. Mahapatra, "Read Range of UHF Passive RFID," *International Journal of Computer Theory and Engineering,* vol. 2, no. 3, pp. 1793-8201, 2010.

[30] T. Björninen, K. Espejo Delzo, L. Ukkonen, A. Elsherbeni and L. Sydänheimo, "Long range metal mountable tag antenna for passive UHF RFID systems," *Proc. IEEE RFID-TA Int. Conf.,* pp. 194-198, 2011.

[31] GS-1, "Regulatory status for using RFID in the UHF spectrum," 25 November 2011. [Online]. Available: http://www.gs1.org/docs/epcglobal/UHF_Regulations.pdf. [Accessed 2012 June 5].

[32] M. Hirvonen, P. Pursula, K. Jaakkola and K. Laukkanen, "Planar Inverted-F Antenan for Rdaio Frequency Identification," *IEEE Electronics Letters,* vol. 40, no. 14, pp. 848-849, 2004.

[33] J. Xi, H. Zhu and T. Ye, "Platform-tolerant PIFA-type UHF RFID tag antenna," *2010 IEEE International Conference on RFID,* pp. 174-180, 2010.

[34] N. Wu, M. Nystrom, T. Lin and H. Yu, "Challenges to global RFID adoption," *Technovation,* vol. 26, no. 12, pp. 1317-1323, 2006.

[35] C. Murray, "Design News -- EDN," 8 June 2006. [Online]. Available: http://www.edn.com/article/464469-RFID_tags_driving_toward_5_cents.php. [Accessed 5 May 2012].

[36] J. Gummeson, P. Zhang and D. Ganesan, "Flit: A Bulk Transmission Protocol for RFID-Scale Sensors," in *roceedings of the 10th International Conference on Mobile Systems, Applications and Services (MobiSys 2012)*, 2012..

[37] S. Garfinkel, A. Juels and R. Pappu, "RFID privacy: an overview of problems and proposed solutions," *IEEE Security & Privacy,* vol. 3, no. 3, pp. 34-43, 2005.

[38] C. Floerkemeier and M. Lampe, "RFID middleware design - addressing application requirements and RFID constraints," in *The Smart Objects and Ambient Intelligence Conference* , 2005.

[39] W. Stutzman and G. Thiele, Antenna Theory and Design, 2nd ed., Hoboken, New Jersey: John Wiley & Sons, Inc., 1998.

[40] C. Balanis, Antenna Theory - Analysis and Design, 3rd ed., Hoboken, New Jersey: John Wiley & Sons, Inc., 2005.

[41] K. Kurokawa, "Power Waves and the Scattering Matrix," *IEEE Transactions on Microwave Theory and Techniques,* vol. 13, no. 2, pp. 194- 202, 1965.

[42] P. Nikitin, K. Rao, S. Lam, V. Pillai, R. Martinez and H. Heinrich, "Power reflection coefficient analysis for complex impedances in RFID tag design," *IEEE Transactions on Microwave Theory and Techniques,* vol. 53, no. 9, pp. 2721- 2725, 2005.

[43] P. Nikitin, K. Rao, R. Martinez and S. Lam, "Sensitivity and Impedance Measurements of UHF RFID Chips," *IEEE Transactions on Microwave Theory and Techniques,* vol. 57, no. 5, pp. 1297-1302, 2009.

[44] G. Marrocco, "The art of UHF RFID antenna design: impedance-matching and size-reduction techniques," *IEEE Antennas and Propagation Magazine,* vol. 50, no. 1, pp. 66-79, 2008.

[45] K. Rao, P. Nikitin and S. Lam, "Antenna design for UHF RFID tags: a review and a practical application," *IEEE Transactions on Antennas and Propagation,* vol. 53, no. 12, pp. 3870- 3876, 2005.

[46] P. Pursula, M. Hirvonen, K. Jaakkola and T. Varpula, "Antenna Effective Aperture

Measurement With Backscattering Modulation," *IEEE Transactions of Antennas and Propagation,* vol. 55, no. 10, pp. 2836-2843, 2207.

[47] P. Pursula, T. Vähä-Heikkilä, A. Müller, D. Neculoiu, G. Konstantinidis, A. Oja and J. Tuovinen, "Millimeter-wave identification - a new short-range radio system for low-power high data-rate applications," *IEEE Transactions on Microwave Theory and Technology,* vol. 56, no. 10, p. 2008, 2221-2228.

[48] P. Nikitin and K. Rao, "Antennas and Propagation in UHF RFID Systems," *2008 IEEE International Conference on RFID,* pp. 277-288, 2008.

[49] P. Foster and R. Burberry, "Antenna problems in RFID systems," *IEE Colloquium on RFID Technology (Ref. No. 1999/123),* pp. 3/1-3/5, 1999.

[50] J. Volakis, K. Fujimoto and C.-C. Chen, Small Antennas: Miniaturization Techniques & Applications, McGraw-Hill , 2010.

[51] K. Lin, S. Chen and R. Mittra, "A Capacitively Coupling Multifeed Slot Antenna for Metallic RFID Tag Design," *IEEE Antennas and Wireless Propagation Letters,* vol. 9, p. 447 – 450, 2010.

[52] W. Zhao, G. Wang and X. La, "Active E-Plate with Slot Antenna," *International Conference on Wireless Communications, Networking and Mobile Computing,* pp. 1-3, 2008.

[53] L. Ukkonen, L. Sydanheimo and M. Kivikoski, "Effects of metallic plate size on the performance of microstrip patch-type tag antennas for passive RFID," *IEEE Antennas and Wireless Propagation Letters,* vol. 4, pp. 410- 413, 2005.

[54] S. Kim, B. Yu, Y.-S. Chung, F. Harackiewicz and B. Lee, "Patch-type radio frequency identification tag antenna mountable on metallic platforms," *Microwave and Optical Technology Letters,* vol. 48, no. 12, pp. 2446-2448, 2006.

[55] G. Kumar and K. Ray, Boradband Microstrip Antennas, Norwood, MA.: Artech House, Inc., 2003.

[56] R. Bhattacharyya, C. Floerkemeier and S. Sarma, "Towards tag antenna based sensing - An RFID displacement sensor," *2009 IEEE International Conference on RFID,* pp. 95-102, 2009.

[57] R. Bhattacharyya, C. Floerkemeier and S. Sarma, "RFID tag antenna based temperature sensing," *2010 IEEE International Conference on RFID,* pp. 8-15, 2010.

[58] G. Marrocco, L. Mattioni and C. Calabrese, "Multiport Sensor RFIDs for Wireless Passive Sensing of Objects—Basic Theory and Early Results," *IEEE Transactions on Antennas and Propagation,* vol. 56, no. 8, pp. 2691-2702, 2008.

[59] S. Johan, X. Zeng, T. Unander, A. Koptyug and H.-E. Nilsson, "Remote Moisture Sensing utilizing Ordinary RFID Tags," *2007 IEEE Sensors,* pp. 308-311, 2007.

[60] S. Caizzone, C. Occhiuzzi and G. Marrocco, "Multi-Chip RFID Antenna Integrating Shape-Memory Alloys for Detection of Thermal Thresholds," *IEEE Transactions on Antennas and Propagation,* vol. 59, no. 7, pp. 2488-2494, 2011.

[61] M. Philipose, J. Smith, B. Jiang, A. Mamishev, S. Roy and K. Sundara-Rajan,

"Battery-free wireless identification and sensing," *IEEE Pervasive Computing,* vol. 4, no. 1, pp. 37- 45, 2005.

[62] I. M. AG, "SL900A EPC Class 3 Sensory Tag Chip - Datasheet," [Online]. Available: http://www.ids-microchip.com/doc/sd/SL900A_SD.pdf. [Accessed 12 June 2012].

[63] J. Yi, M. Law, Y. Ling, M. C. Lee, K. P. Ng, B. Gao, H. Luong, A. Bermak, M. Chan, W.-H. Ki, C.-Y. Tsui and M. Yuen, "A System-on-Chip EPC Gen-2 Passive UHF RFID Tag With Embedded Temperature Sensor," *IEEE Journal of Solid-State Circuits,* vol. 45, no. 11, pp. 2404-2420, 2010.

[64] M. Law, A. Bermak and H. Luong, "A Sub-uW Embedded CMOS Temperature Sensor for RFID Food Monitoring Application," *IEEE Journal of Solid-State Circuits,* vol. 45, no. 6, pp. 1246-1255, 2010.

[65] A. Sample, D. Yeager, P. Powledge, A. Mamishev and J. Smith, "Design of an RFID-Based Battery-Free Programmable Sensing Platform," *IEEE Transactions on Instrumentation and Measurement,* vol. 57, no. 11, pp. 2608-2615, 2008.

[66] G. Marrocco, "Pervasive electromagnetics: sensing paradigms by passive RFID technology," *IEEE Wireless Communications,* vol. 17, no. 6, pp. 10-17, 2010.

[67] A. Rida, L. Yang and M. Tentzeris, RFID-Enabled Sensor Design and Applications, Boston: Artech House, 2010.

[68] C. Occhiuzzi and G. Marrocco, "Pervasive Body Sensing: Implanted RFID Tags for Vascular Monitoring," *IEEE Antennas and Propagation Symposium,* 2010.

[69] E. Jones, M. Henry and D. Cochran, "RFID Pharmaceutical Tracking: From Manufacturer Through In Vivo Drug Delivery," *Journal of Medical Devices,* vol. 4, no. 1, 2010.

[70] J. Dowling, M. Tentzeris and N. Beckett, "RFID-enabled temperature sensing devices: A major step forward for energy efficiency in home and industrial applications?," *IEEE MTT-S International Microwave Workshop on Wireless Sensing, Local Positioning, and RFID,* pp. 24-25, 2009.

[71] J. Dowling and M. Tentzeris, "'smart house" and "smart-energy" applications of low-power RFID-based wireless sensors," *Asia Pacific Microwave Conference,* pp. 2412-2415, 2009.

[72] J. Koch, J. Wettach, E. Bloch and K. Berns, "Indoor Localisation of Humans, Objects, and mobile Robots with RFID Infrastructure," *7th International Conference on Hybrid Intelligent Systems,* pp. 271-276, 2007.

[73] M. Buettner, R. Prasad, M. Philipose and D. Wetherall, "Recognizing daily activities with RFID-based sensors," *Proceedings of the 11th international conference on Ubiquitous computing,* 2009.

[74] J. Yang, J. Lee and J. Choi, "Activity Recognition Based on RFID Object Usage for Smart Mobile," *JOURNAL OF COMPUTER SCIENCE AND TECHNOLOGY,* vol. 26, no. 2, pp. 239-246, 2011.

[75] R. Rusu, B. Gerkey and M. Beetz, "Robots in the kitchen: Exploiting ubiquitous sensing and actuation," *Robotics and Autonomous Systems Journal (Special Issue*

on Network Robot Systems), 2008.

[76] G. Marrocco and F. Amato, "Self-sensing passive RFID: From theory to tag design and experimentation," *European Microwave Conference,* pp. 1-4, 2009.

[77] S. Merilampi, P. Ruuskanen, T. Björninen, L. Ukkonen and L. Sydänheimo, "Printed passive UHF RFID tags as wearable strain sensors," *3rd International Symposium on Applied Sciences in Biomedical and Communication Technologies,* pp. 1-5, 2010.

[78] R. Dai and C. Young, "Theory and sensing applications of a long antenna on layered media," *Radio Science,* vol. 32, no. 1, pp. 43-57, 1997.

[79] Y.-J. Ren and K. Chang, "Bow-tie retrodirective rectenna," *IEEE Electronics Letters,* vol. 42, no. 4, pp. 191- 192, 2006.

[80] M. Trotter, C. Valenta, G. Koo, B. Marshall and G. Durgin, "Multi-antenna techniques for enabling passive RFID tags and sensors at microwave frequencies," *2012 IEEE International Conference on RFID,* pp. 1-7, 2012.

[81] A. Ralston, C. Klein, P. Thoma and D. Denton, "Amodel for the relativeenvironmentalstability of aseries of polyimidecapacitancehumiditysensors," *Sensors and Actuators B: Chemical,* vol. 34, no. 1-3, pp. 343-348, 1996.

[82] L. Greenspan, "Humidity fixed points of binary saturated aqueous solutions," *A Physics and Chemistry Journal of Research of the National Bureau of Standards,* vol. 81A, no. 1, pp. 89-96, 1977.

[83] U. Kaatze, "Complex permittivity of water as a function of frequency and temperature," *J. Chem. Eng. Data,* vol. 34, no. 4, p. 371–374, 1989.

[84] L. Ukkonen and L. Sydänheimo, "Threshold Power-based Radiation Pattern Measurement of Passive UHF RFID Tags," *PIERS Online,* vol. 6, no. 6, pp. 523- 526, 2010.

[85] C. Floerkemeier, M. Lampe, A. Ferscha and F. Mattern, "Issues with RFID Usage in Ubiquitous Computing Applications," in *Lecture Notes in Computer Science: Pervasive Computing*, Berlin / Heidelberg, Springer, 2004, pp. 188-193.

[86] K. Hon, L. Li and I. Hutchings, "Direct writing technology—Advances and developments," *CIRP Annals - Manufacturing Technology,* vol. 57, no. 2, p. 601– 620, 2008.

[87] H. Lee, K. Chou and K. Huang, "Inkjet printing of nanosized silver colloids," *Nanotechnology,* vol. 16, no. 10, 2005.

[88] K. Bong, K. Dongjo, J. Sunho, M. Jooho and S. Jang, "Directwriting of copper conductive patterns by ink-jetprinting," *Thin Solid Films,* vol. 515, no. 19, p. 7706– 7711, 2007.

[89] S. Ko, H. Pan, C. Grigoropoulos, C. Luscombe, J. Fréchet and P. Poulikakos, "All-inkjet-printed flexible electronics fabrication on a polymer substrate by low-temperature high-resolution selective laser sintering of metal nanoparticles," *Nanotechnology,* vol. 18, no. 34, 2007.

[90] J. Greer and R. Street, "Thermal cure effects on electrical performance of

nanoparticle silver inks," *Acta Materialia,* vol. 55, no. 18, pp. 6345-6349, 2007.

[91] Harima Chemicals, "NanoPaste NPS-JL datasheet," [Online]. Available: http://www.harima.co.jp/en/products/pdf/16-17e.pdf. [Accessed 18 May 2012].

[92] Cabot Corporation, "CCI-300 Data Sheet," [Online]. Available: http://www.cabot-corp.com/wcm/download/en-us/nb/ATTH4YZ5.doc. [Accessed 29 May 2012].

[93] V. Ubramanian, J. Frechet, P. Chang, D. Huang, J. Lee, S. Molesa, A. Murphy, D. Redinger and S. Volkman, "Progress Toward Development of All-Printed RFID Tags: Materials, Processes, and Devices," *Proceedings of the IEEE,* vol. 93, no. 7, pp. 1330-1338, 2005.

[94] D. Pozar, Microwave Engineering, New York: Wiley, 2007.

[95] S. Wentwhorth, Fundamentals of electromagnetics with engineering applications, Wiley, 2005.

[96] Y. Iwashita, "Reduction of RF power loss caused by skin effect," *Lecture Notes in Computer Science,* vol. 5103, pp. 700-702, 2004.

[97] M. Mäntysalo, P. Mansikkamäki and J. e. a. Miettinen, "Evaluation of inkjet technology for electronic packaging and system integration," *Proceedings of the 57th Electronic Components and Technology conference,* pp. 89-94, 2007.

[98] J. Virtanen, T. Björninen, L. Ukkonen, K. Kaija, T. Joutsenoja, L. Sydänheimo and A. Z. Elsherbeni, "The effect of conductor thickness in passive inkjet printed RFID tags," *2010 IEEE Antennas and Propagation Society International Symposium,* pp. 1-4, 2010.

[99] J. Siden, T. Olsson, A. Koptioug and H. Nilsson, "Reduced amount of conductive ink with gridded printed antennas," *Proceedings of the 5th international conference on polymers and adhesives in microelectronics and photonics ,* pp. 86-89, 2005.

[100] T. Björninen, A. Elsherbeni and L. Ukkonen, "Performance of single and double T-matched short dipole tag antennas for UHF RFID systems," *Journal of Applied Computational Electromagnetics Society,* vol. 26, no. 12, pp. 953-962, 2011.

[101] E. Koski, K. Koski, L. Ukkkonen, L. Sydanheimo, J. Virtanen, T. Bjorninen and A. Elsherbeni, "Performance of inkjet-printed narrow-line passive UHF RFID tags on different objects," *2011 IEEE International Symposium on Antennas and Propagation,* pp. 537-540, 2011.

[102] Global Industry Analysts, Inc., "Plywood: A Global Strategic Business Report," 2010.

[103] C. Medeiros, J. Costa and C. Fernandes, "RFID Smart Shelf With Confined Detection Volume at UHF," *IEEE Antennas and Wireless Propagation Letters,* vol. 7, pp. 773-776, 2008.

[104] E. Becker, V. Metsis, R. Arora, J. Vinjumur, Y. Xu and F. Makedon, "SmartDrawer: RFID-Based Smart Medicine Drawer for Assistive," *Proc. 2nd International Conference on Pervsive Technologies Related to Assistive Environments,* pp. 258-263, 2008.

[105] Finnish Forest Industries Federation, Handbook of Finnish Plywood, Lahti: